Downlink Average Rate and SINR Distribution in Cellular Networks

Xiaojun Yan, Jing Xu, Yuanping Zhu, Jiang Wang, Yang Yang, *Senior Member, IEEE*, and Cheng-Xiang Wang, *Senior Member, IEEE*

***Abstract*—The statistical characteristics of the signal-to-interference plus noise ratio (SINR) are closely related to many performance metrics of cellular networks. In this paper, the downlink average rate and SINR distribution are studied for orthogonal frequency division multiple access (OFDMA)-based cellular networks subject to the distance-dependent path loss and shadow fading (SF). With the analytical approximate mean and moment generating function (MGF) of the SINR in the logarithmic domain, the closed-form approximation for the lower and upper bounds of the average rate is obtained. Then the distribution of the SINR in the logarithmic domain is proposed to be approximated as the normal inverse Gaussian (NIG) distribution whose parameters are computed explicitly through moment matching. Also, the closed-form expression for the cumulative distribution function (CDF) of the SINR based on the NIG approximation is derived. Simulation results not only verify the tightness of the bounds, but also show that the NIG approximation is up to one order of magnitude more accurate than the Pearson type IV approximation and at least one order of magnitude more accurate than the lognormal approximation when the SF correlation coefficient is small or the standard deviations of the SF are large or different.**

***Index Terms*—Cumulative distribution function, normal inverse Gaussian distribution, orthogonal frequency division multiple access, signal to interference plus noise ratio, statistical characteristics.**

I. Introduction

THE statistical characteristics of the signal to interference plus noise ratio (SINR) are closely related to many important performance metrics of cellular networks, such as the average rate and outage probability. In orthogonal frequency division multiple access (OFDMA)-based cellular networks, as there is no intra-cell interference, the SINR is the ratio of the signal to the inter-cell interference plus noise. In emerging cellular networks [1]–[3], base stations (BSs) will be more and more densely deployed, thus the inter-cell interference will be more and more intense. Investigation of the statistical characteristics of the SINR is critical for the analysis and optimization of the network performance.

So far, there have been several approaches proposed to study the statistical characteristics of the SINR in cellular networks. In code division multiple access networks, the approximate SINR distribution is investigated in [4] based on the Gaussian approximation to the multi-user interference plus noise. Unfortunately, unlike code division multiple access networks, the inter-cell interference in OFDMA-based cellular networks cannot be simply approximated as a Gaussian random variable (RV) since the interference is narrowband and the number of interferers is finite. This makes it more complicated to investigate the statistical characteristics of the SINR in OFDMA-based cellular networks. Recently, based on the assumption [5] that BSs are distributed according to the Poisson point process, the outage probability, SINR distribution, average rate and rate distribution have been studied. The outage probability derived in [6], [7] is closed-form only when there is no noise or the path loss exponent is 4, and there are no closed-form expressions for the SINR distribution [8], average rate [6], [7], [9] and rate distribution [10]. Some researchers have studied the statistical characteristics of the SINR in planned cellular networks [11]–[14]. For networks without fading, the rate distribution and average rate are analyzed in [15] based on the derived closed-form distance distribution between BSs and user equipments (UEs). There is no closed-form expression for the average rate. In [16], as the approximation to the n-th order original moment of the SINR, the ratio of the n-th order original moment of the signal to that of the interference plus noise is analyzed. For networks undergoing the lognormal shadow fading (SF), this ratio is given in closed form based on the Gauss-Hermite approximation [17], [18] to the moment generating function (MGF) of the interference plus noise. Nevertheless, simulation results in [16] showed that this ratio cannot approximate the moments of the SINR well when the number of the interferers is small.

One of the main challenges for the statistical modeling of the SINR is the statistical modeling of the inter-cell interference. For networks undergoing the lognormal SF, the inter-cell interference is the sum of several lognormal RVs. The modeling of

Manuscript received May 1, 2015; revised September 22, 2015 and December 5, 2015; accepted December 8, 2015. Date of publication December 22, 2015; date of current version February 12, 2016. This work is partially sponsored by the International Science and Technology Cooperation Program of China under grant 2014DFE10160, the National Natural Science Foundation of China (NSFC) under grant 61471347, the Science and Technology Commission of Shanghai Municipality (STCSM) under grant 15511103200, the National Science and Technology Major Project under grant 2015ZX03002004 and the EU FP7 QUICK project under grant PIRSES-GA-2013-612652. Part of this paper was presented at the IEEE International Conference on Communications (ICC), London, U.K., June 2015. The associate editor coordinating the review of this paper and approving it for publication was M. DiRenzo. *(Corresponding author: Yang Yang.)*

X. Yan, J. Xu, Y. Zhu, J. Wang, and Y. Yang are with the Key Laboratory of Wireless Sensor Network and Communication, Shanghai Institute of Microsystem and Information Technology (SIMIT), Chinese Academy of Sciences (CAS), Shanghai 200050, China, and also with Shanghai Research Center for Wireless Communications(WiCO), Shanghai 201210, China (e-mail: xiaojun.yan@wico.sh; jing.xu@wico.sh; yuanping.zhu@wico.sh; jiang.wang@wico.sh; yang.yang@wico.sh).

C.-X. Wang is with the Institute of Sensors, Signals, and Systems, School of Engineering and Physical Sciences, Heriot-Watt University, Edinburgh EH14 4AS, U.K. (e-mail: cheng-xiang.wang@hw.ac.uk).

Digital Object Identifier 10.1109/TCOMM.2015.2511014

the lognormal sum is a long-standing problem and exact closed-form expressions for the lognormal sum distribution remain unknown. So far, several approximation approaches have been proposed to study the statistical characteristics of the lognormal sum, including lognormal approximations [19]–[21], Pearson type IV approximations [22]–[25], MGF-based approximations [17], [26], [27] and other approximation methods [28], [29]. However, none of these methods satisfies the following two properties simultaneously: 1) accurate in the whole region of the cumulative distribution function (CDF); and 2) parameters of the approximate distribution can be computed explicitly. For cellular networks, it is desirable to obtain the closed-form expressions for the average rate and statistical characteristics of the SINR for general cases, and there is no accurate approximate SINR distribution whose parameters can be presented analytically.

In the field of finance, the normal inverse Gaussian (NIG) distribution has been used in [30] to approximate the distribution of a stochastic process. Fortunately, the parameters of the NIG distribution can be explicitly expressed in terms of the mean, variance, skewness, and kurtosis. In this paper, the lower and upper bounds of the downlink average rate and distribution of the downlink SINR are studied for OFDMA-based cellular networks considering the distance-dependent path loss and SF. The closed-form approximation for the lower and upper bounds of the average rate is obtained from the statistical characteristics of the SINR in the logarithmic domain, and the NIG distribution is proposed to approximate the distribution of the SINR in the logarithmic domain. To the best of our knowledge, no published literature presents a closed-form bound of the average rate or considers the NIG approximation to the distribution of the SINR. First, the analytical approximate mean and MGF of the SINR in the logarithmic domain are given. Further, the lower bound of the average rate is presented through the mean of the SINR in the logarithmic domain. The average rate is proved to be upper bounded by the certain value of the MGF of the SINR in the logarithmic domain. With the analytical approximate mean and MGF, the closed-form approximation for the lower and upper bounds of the average rate can be obtained. Then the NIG approximation to the distribution of the SINR in the logarithmic domain is elaborated. Using the moment matching method, the parameters of the NIG approximation are computed explicitly through the closed-form approximation for the mean, variance, skewness and kurtosis of the SINR in the logarithmic domain. The closed-form expression for the CDF of the SINR based on the NIG approximation is also given in terms of exponential functions and error functions. Finally, simulation results verify that the closed-form approximation for the lower and upper bounds of the average rate is tight. In addition, it is shown that the NIG approximation outperforms the lognormal approximation and Pearson type IV approximation especially when the SF correlation coefficient is small or the standard deviations of the SF are large or different. Also, it is verified that the CDF of the SINR based on the NIG approximation can always get the satisfactory performance. The main contributions of this paper are as follows.

1) The closed-form approximation for the lower and upper bounds of the average rate is presented. The lower bound is dependent on the approximate mean of the SINR in the logarithmic domain, and the upper bound is determined by the certain value of the approximate MGF of the SINR in the logarithmic domain.
2) The distribution of the SINR in the logarithmic domain is proposed to be approximated as the NIG distribution whose parameters are computed explicitly. Also, the closed-form expression for the CDF of the SINR based on the NIG approximation is given in terms of exponential functions and error functions.

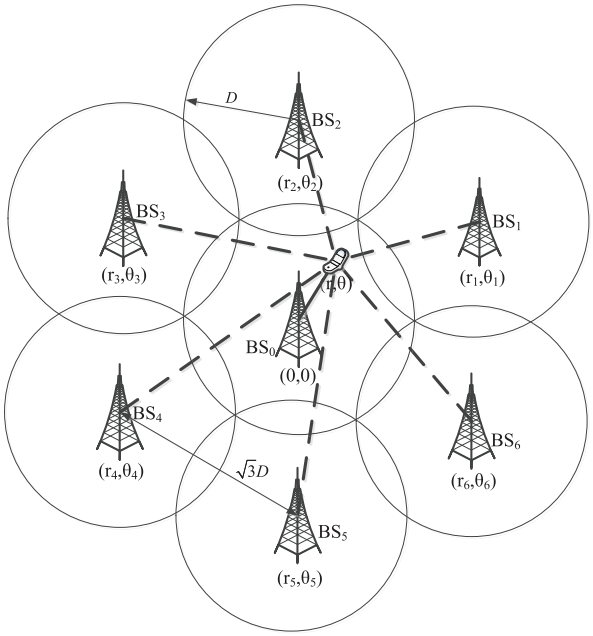

Fig. 1. Two-dimensional OFDMA-based cellular network model.

The rest of this paper is organized as follows. Section II gives the system model and problem formulation. In Section III, the closed-form approximation for the lower and upper bounds of the average rate is obtained. Section IV elaborates the NIG approximation to the distribution of the SINR in the logarithmic domain and presents the closed-form expression for the CDF of the SINR based on the NIG approximation. In Section V, numerical experiments are conducted to verify the analysis in this paper. Finally, the paper is concluded in Section VI.

II. System Model and Problem Formulation

In Fig. 1, the two-dimensional layout of an OFDMA-based cellular network is depicted, where the polar coordinate system is used to describe node locations. Without loss of generality, the serving cell and its first-tier interfering cells are shown. The coverage of each cell is considered as a circle with the radius D, and the inter-site distance (ISD) is $\sqrt{3}D$. The BS BS_0 of the serving cell locates at the origin, and its connected UE locates at (r, θ). The location of BS_i (i.e., the BS of the i-th interfering cell) is denoted as (r_i, θ_i), $i = 1, \ldots, L$. Each BS is equipped with an omnidirectional antenna. The UE in the serving cell receives the useful signal from BS_0 and suffers the downlink inter-cell interference from the L interfering cells. The corresponding useful link is denoted as the bold solid line, and

the corresponding interfering links are represented as the bold dashed lines.

For the UE located at (r, θ), the distance between the UE and BS_i $(i = 0, \ldots, L)$ is

$$d_i = \begin{cases} r, & i = 0, \\ \sqrt{r^2 + r_i^2 - 2rr_i \cos(\theta - \theta_i)}, & i = 1, \ldots, L. \end{cases} \quad (1)$$

The signal power received from BS_i can be given by

$$Y_i = P_t G_b A d_i^{-\eta} \exp(\xi X_i) = 10^{(\mu_i + X_i)/10}, \quad (2)$$

where $\xi = \ln 10 \,/ 10$, $\mu_i = 10 \lg \left(P_t G_b A d_i^{-\eta} \right)$, P_t and G_b are the transmit power and antenna gain of each BS, respectively, η is the path loss exponent, A is the path loss constant, and X_i is the SF of the corresponding communication link. Generally, X_i is considered as a zero-mean Gaussian RV whose standard deviation is σ_idB. From (2), it can be seen that Y_i is a lognormal RV which can be denoted as $LN(\xi\mu_i, \xi\sigma_i)$. The distribution of Y_i is defined as

$$f_{Y_i}(y_i) = \frac{1}{\sqrt{2\pi}(\xi\sigma_i) y_i} \exp\left[-\frac{(\ln y_i - \xi\mu_i)^2}{2(\xi\sigma_i)^2} \right]. \quad (3)$$

The total downlink inter-cell interference power received by the UE can be obtained from

$$Y_I = \sum_{i=1}^{L} Y_i = \sum_{i=1}^{L} 10^{(\mu_i + X_i)/10}. \quad (4)$$

This means that Y_I is the sum of several lognormal RVs. The background noise [26] at the UE is

$$N_b = hTB\varphi,$$

where h is the Boltzmann constant, T is the ambient temperature in Kelvin, B is the channel bandwidth, and φ is the noise figure of the UE.

Denoting the SINR for the UE as the RV Y

$$Y = \frac{Y_0}{Y_I + N_b} = \frac{10^{(\mu_0 + X_0)/10}}{\sum_{i=1}^{L} 10^{(\mu_i + X_i)/10} + N_b}, \quad (5)$$

the SINR in the logarithmic domain for the UE can be given by

$$Z = \ln Y = \ln Y_0 - \ln(Y_I + N_b) = Z_1 - Z_2, \quad (6)$$

where

$$Z_1 = \ln Y_0 = \xi\mu_0 + \xi X_0, \quad (7a)$$

$$Z_2 = \ln(Y_I + N_b) = \ln\left[\sum_{i=1}^{L} 10^{(\mu_i + X_i)/10} + N_b \right]. \quad (7b)$$

Z_1 is a Gaussian RV with the mean $\xi\mu_0$ and variance $(\xi\sigma_0)^2$.

When the SF RVs X_i $(i = 0, \ldots, L)$ are independent from each other, the MGF and n-th order cumulant of Z are given in Lemma 1.

Lemma 1: When X_i is independent from each other, the MGF of Z can be expressed as

$$M_Z(s) = \exp\left[-(\xi\mu_0)s + \frac{1}{2}(\xi\sigma_0)^2 s^2 \right] M_{Z_2}(-s), \quad (7)$$

where $M_{Z_2}(s) = E\left[e^{-sZ_2}\right]$ is the MGF of Z_2. The n-th order cumulant of Z can be obtained from

$$c_Z^{(1)} = \xi\mu_0 - c_{Z_2}^{(1)}, \quad (9a)$$

$$c_Z^{(2)} = (\xi\sigma_0)^2 + c_{Z_2}^{(2)}, \quad (9b)$$

$$c_Z^{(n)} = (-1)^n c_{Z_2}^{(n)}, \ n > 2, \quad (9c)$$

where $c_{Z_2}^{(n)}$ is the n-th order cumulant of Z_2.

Proof: The MGF of Z_1 is

$$M_{Z_1}(s) = E\left[e^{-sZ_1}\right] = \exp\left[-(\xi\mu_0)s + \frac{1}{2}(\xi\sigma_0)^2 s^2 \right]. \quad (10)$$

As Z_1 and Z_2 are independent from each other, the MGF of Z can be expressed as

$$\begin{aligned} M_Z(s) &= E\left[e^{-s(Z_1 - Z_2)}\right] \\ &= E\left[e^{-sZ_1}\right] E\left[e^{sZ_2}\right] \\ &= M_{Z_1}(s) M_{Z_2}(-s). \end{aligned} \quad (11)$$

Substituting (10) into (11), (8) can be obtained. According to [31], the n-th order cumulant of Z can be given by

$$c_Z^{(n)} = c_{Z_1}^{(n)} + (-1)^n c_{Z_2}^{(n)} \quad (12)$$

For Z_1, there are only two non-zero cumulants, i.e., the mean $\xi\mu_0$ and variance $(\xi\sigma_0)^2$. This yields (9). ■

As the first cumulant is equal to the mean for an RV, (9a) can be rewritten as

$$m_Z^{(1)} = \xi\mu_0 - m_{Z_2}^{(1)}, \quad (13)$$

where $m_Z^{(1)}$ and $m_{Z_2}^{(1)}$ are the mean of Z and Z_2, respectively.

When the SF RVs are correlated, X_i can be expressed as [32]

$$X_i = \sigma_i \sqrt{1 - \zeta} W_i + \sigma_i \sqrt{\zeta} S_0, \quad (14)$$

where ζ is the correlation coefficient, W_i and S_0 are independent Gaussian variables with zero mean and unit variance. For different BSs, W_i is independent from each other, while S_0 keeps the same. The first and second part of the right hand side of (14) can be considered as the independent and correlated component of X_i, respectively. In interference-limited networks, when the SF RVs are correlated and the standard deviations of the SF of interfering links are the same, the MGF and n-th order cumulant of Z are given in Lemma 2.

Lemma 2: In interference-limited networks, when the SF RVs are correlated and $X_i (i = 1, \ldots, L)$ have the same standard deviation σ_IdB, the MGF of Z can be expressed as

$$M_Z(s) = \exp\left[\eta s \ln r + \frac{1}{2}\xi^2 s^2 \left(\sigma_0^2 - 2\zeta\sigma_0\sigma_I + \zeta\sigma_I^2 \right) \right] \cdot M_{Z_2'}(-s), \quad (15)$$

where

$$Z_2' = \ln\left[\sum_{i=1}^{L} d_i^{-\eta} \exp\left(\xi\sigma_I\sqrt{1-\zeta}W_i\right)\right], \tag{16}$$

and $M_{Z_2'}(s)$ is the MGF of Z_2'. The n-th order cumulant of Z can be obtained from

$$c_Z^{(1)} = -\eta\ln r - c_{Z_2'}^{(1)}, \tag{17a}$$

$$c_Z^{(2)} = \xi^2\left(\sigma_0^2 - 2\zeta\sigma_0\sigma_I + \zeta\sigma_I^2\right) + c_{Z_2'}^{(2)}, \tag{17b}$$

$$c_Z^{(n)} = (-1)^n c_{Z_2'}^{(n)},\ n > 2, \tag{17c}$$

where $c_{Z_2'}^{(n)}$ is the n-th order cumulant of Z_2'.

Proof: For interference-limited networks, the background noise N_b can be neglected, thus the SINR in the logarithmic domain can be expressed as

$$\begin{aligned} Z &= \xi\mu_0 + \xi X_0 - \ln\left[\sum_{i=1}^{L} 10^{(\mu_i+X_i)/10}\right] \\ &= -\eta\ln r + \xi X_0 - \ln\left(\sum_{i=1}^{L} d_i^{-\eta} 10^{X_i/10}\right). \end{aligned} \tag{18}$$

When σ_i $(i = 1, \ldots, L)$ have the same value σ_I, according to (14), (18) can be rewritten as

$$\begin{aligned} Z &= -\eta\ln r + \xi\left(\sigma_0\sqrt{1-\zeta}W_0 + \sigma_0\sqrt{\zeta}S_0\right) \\ &\quad - \ln\left[\sum_{i=1}^{L} d_i^{-\eta} 10^{\left(\sigma_I\sqrt{1-\zeta}W_i + \sigma_I\sqrt{\zeta}S_0\right)/10}\right] \\ &= -\eta\ln r + \xi\sigma_0\sqrt{1-\zeta}W_0 + \xi\sqrt{\zeta}\left(\sigma_0 - \sigma_I\right)S_0 \\ &\quad - \ln\left[\sum_{i=1}^{L} d_i^{-\eta} 10^{\sigma_I\sqrt{1-\zeta}W_i/10}\right] \\ &= Z_1' - Z_2', \end{aligned} \tag{19}$$

where

$$Z_1' = -\eta\ln r + \xi\sigma_0\sqrt{1-\zeta}W_0 + \xi\sqrt{\zeta}\left(\sigma_0 - \sigma_I\right)S_0. \tag{20}$$

It can be seen that Z_1' is a Gaussian RV with the mean $-\eta\ln r$ and variance $\xi^2\left(\sigma_0^2 - 2\zeta\sigma_0\sigma_I + \zeta\sigma_I^2\right)$. The MGF of Z_1' is

$$M_{Z_1'}(s) = \exp\left[\eta s\ln r + \frac{1}{2}\xi^2 s^2\left(\sigma_0^2 - 2\zeta\sigma_0\sigma_I + \zeta\sigma_I^2\right)\right]. \tag{21}$$

Furthermore, Z_1' is independent from Z_2'. Thus the MGF and n-th order cumulant of Z can be expressed as (15) and (17), respectively. ■

When σ_0 and σ_I have the same value σ, the correlated component in Z can be eliminated. In this case, when the standard deviation σ of X_i $(i = 0, \ldots, L)$ is fixed and the SF correlation coefficient ζ increases, the standard deviation $\sigma\sqrt{1-\zeta}$ of the independent component W_i decreases. This means the increase of the SF correlation coefficient is equivalent to the decrease of the standard deviation of the SF RVs. Thus the impact of the SF correlation coefficient on the SINR is opposite to that of the standard deviation of the SF when all the communication links have the same standard deviation of the SF. (17a) can be rewritten as

$$m_Z^{(1)} = -\eta\ln r - m_{Z_2'}^{(1)}, \tag{22}$$

where $m_{Z_2'}^{(1)}$ is the mean of Z_2'.

III. Lower and Upper Bounds of Average Rate

In this section, the approximate mean and MGF of the SINR in the logarithmic domain Z are given and utilized to obtain the lower and upper bounds of the average rate. The computation of the exact mean and MGF of Z involves the multi-fold integration. In order to derive the bounds of the average rate, the Gauss-Hermite Quadrature [17], [23] is exploited to obtain the approximate expression for the multi-fold integration.

A. Approximate Mean and MGF of SINR in Logarithmic Domain

When the SF RVs X_i $(i = 0, \ldots, L)$ are independent from each other, the approximate mean and MGF of Z are given in Theorem 1.

Theorem 1: When X_i $(i = 0, \ldots, L)$ are independent from each other, the approximate mean and MGF of Z can be respectively expressed as

$$\begin{aligned} \hat{m}_Z^{(1)} &= \xi\mu_0 - \left(\frac{1}{\sqrt{\pi}}\right)^L \sum_{n_1=1}^{N_1}\cdots\sum_{n_L=1}^{N_L}\left(\prod_{i=1}^{L}\omega_{n_i}\right) \\ &\quad \cdot\ln\left[\sum_{i=1}^{L}\kappa_{n_i}\left(a_{n_i};\mu_i,\sigma_i\right) + N_b\right], \end{aligned} \tag{23a}$$

$$\begin{aligned} \hat{M}_Z(s) &= \left(\frac{1}{\sqrt{\pi}}\right)^L \sum_{n_1=1}^{N_1}\cdots\sum_{n_L=1}^{N_L}\left(\prod_{i=1}^{L}\omega_{n_i}\right) \\ &\quad \cdot\exp\left[\left\{\ln\left[\sum_{i=1}^{L}\kappa_{n_i}\left(a_{n_i};\mu_i,\sigma_i\right) + N_b\right]\right. \right. \\ &\quad \left.\left. - \left(\xi\mu_0\right)\right\}s + \frac{1}{2}\left(\xi\sigma_0\right)^2 s^2\right], \end{aligned} \tag{23b}$$

where ω_{n_i} and a_{n_i} are the corresponding weights and abscissas, N_i $(i = 1, \ldots, L)$ is the order of the Hermite integration, and $\kappa_{n_i}\left(a_{n_i};\mu_i,\sigma_i\right) = 10^{\left(\sqrt{2}\sigma_i a_{n_i} + \mu_i\right)/10}$. The weights and abscissas are constants that can be found in [18] for N up to 20.

Proof: From [23], the approximate MGF of the total downlink inter-cell interference Y_I in the logarithmic domain can be obtained. With a slight modification to take the background noise into consideration, the approximate MGF of the interference plus noise in the logarithmic domain Z_2 can be expressed as

$$\hat{M}_{Z_2}(s) = \left(\frac{1}{\sqrt{\pi}}\right)^L \sum_{n_1=1}^{N_1} \cdots \sum_{n_L=1}^{N_L} \left(\prod_{i=1}^{L} \omega_{n_i}\right) \cdot \left[\sum_{i=1}^{L} \kappa_{n_i}\left(a_{n_i}; \mu_i, \sigma_i\right) + N_b\right]^{-s}. \quad (24)$$

Based on (24), the approximate mean of Z_2 can be obtained from

$$\hat{m}_{Z_2}^{(1)} = -\left.\frac{d\hat{M}_{Z_2}(s)}{ds}\right|_{s=0} = \left(\frac{1}{\sqrt{\pi}}\right)^L \sum_{n_1=1}^{N_1} \cdots \sum_{n_L=1}^{N_L} \left(\prod_{i=1}^{L} \omega_{n_i}\right) \cdot \ln\left[\sum_{i=1}^{L} \kappa_{n_i}\left(a_{n_i}; \mu_i, \sigma_i\right) + N_b\right]. \quad (25)$$

Replacing $c_{Z_2}^{(1)}$ and $M_{Z_2}(s)$ in Lemma 1 with $\hat{m}_{Z_2}^{(1)}$ and $\hat{M}_{Z_2}(s)$, respectively, (23) can be obtained. ■

In interference-limited networks, when the SF RVs are correlated and the standard deviations of the SF of interfering links are the same, the approximate mean and MGF of Z are given in Theorem 2.

Theorem 2: In interference-limited networks, when $X_i (i = 0, \ldots, L)$ are correlated and $X_i (i = 1, \ldots, L)$ have the same standard deviation σ_IdB, the approximate mean and MGF of Z can be respectively expressed as

$$\hat{m}_Z^{(1)} = -\eta \ln r - \left(\frac{1}{\sqrt{\pi}}\right)^L \sum_{n_1=1}^{N_1} \cdots \sum_{n_L=1}^{N_L} \left(\prod_{i=1}^{L} \omega_{n_i}\right) \cdot \ln\left[\sum_{i=1}^{L} \kappa_{n_i}\left(a_{n_i}; -10\eta \lg d_i, \sigma_I\sqrt{1-\zeta}\right)\right], \quad (26a)$$

$$\hat{M}_Z(s) = \left(\frac{1}{\sqrt{\pi}}\right)^L \sum_{n_1=1}^{N_1} \cdots \sum_{n_L=1}^{N_L} \left(\prod_{i=1}^{L} \omega_{n_i}\right) \cdot \exp\left\{\frac{1}{2}\xi^2 s^2\left(\sigma_0^2 - 2\zeta\sigma_0\sigma_I + \zeta\sigma_I^2\right) + \eta s \ln r + s \ln\left[\sum_{i=1}^{L} \kappa_{n_i}\left(a_{n_i}; -10\eta \lg d_i, \sigma_I\sqrt{1-\zeta}\right)\right]\right\}. \quad (26b)$$

Proof: From (16), Z_2' is the sum of several independent lognormal RVs. For the i $(i = 1, \ldots, L)$-th component lognormal RV, the logarithmic mean and standard deviation are $-\eta \ln d_i$ and $\xi\sigma_I\sqrt{1-\eta}$, respectively. According to [23], the approximate MGF of Z_2' can be expressed as

$$\hat{M}_{Z_2'}(s) = \left(\frac{1}{\sqrt{\pi}}\right)^L \sum_{n_1=1}^{N_1} \cdots \sum_{n_L=1}^{N_L} \left(\prod_{i=1}^{L} \omega_{n_i}\right) \cdot \left[\sum_{i=1}^{L} \kappa_{n_i}\left(a_{n_i}; -10\eta \lg d_i, \sigma_I\sqrt{1-\zeta}\right)\right]^{-s}. \quad (27)$$

Thus the approximate mean of Z_2' can be given by

$$\hat{m}_{Z_2'}^{(1)} = \left(\frac{1}{\sqrt{\pi}}\right)^L \sum_{n_1=1}^{N_1} \cdots \sum_{n_L=1}^{N_L} \left(\prod_{i=1}^{L} \omega_{n_i}\right) \cdot \ln\left[\sum_{i=1}^{L} \kappa_{n_i}\left(a_{n_i}; -10\eta \lg d_i, \sigma_I\sqrt{1-\zeta}\right)\right]. \quad (28)$$

Replacing $c_{Z_2'}^{(1)}$ and $M_{Z_2'}(s)$ in Lemma 2 with $\hat{m}_{Z_2'}^{(1)}$ and $\hat{M}_{Z_2'}(s)$, respectively, (26) can be obtained. ■

B. Lower and Upper Bounds

Since the channel bandwidth is a constant in this paper, investigating the average rate is equivalent to studying

$$R = E\left[\ln\left(1 + e^Z\right)\right] = \int_{-\infty}^{+\infty} \ln\left(1 + e^z\right) f_Z(z)\, dz, \quad (29)$$

where $f_Z(z)$ is the distribution of Z.

The approximate lower bound of the average rate is given in Theorem 3.

Theorem 3: The approximate lower bound of R can be expressed as

$$\hat{R}_L = \ln\left[1 + \exp\left(\hat{m}_Z^{(1)}\right)\right]. \quad (30)$$

Proof: Let $p(z) = \ln(1 + e^z)$. As the second derivative of $p(z)$ is

$$p''(z) = \frac{e^{-z}}{\left(1 + e^{-z}\right)^2} > 0, \quad (31)$$

$p(z)$ is strictly convex. By the Jensen's inequality [33], the lower bound of R can be obtained from

$$R \geq R_L = \ln\left[1 + \exp\left(\int_{-\infty}^{+\infty} z f_Z(z)\, dz\right)\right]. \quad (32)$$

Replacing the mean of Z with $\hat{m}_Z^{(1)}$, (30) can be obtained. ■

Note that $\hat{R}_L$ is only determined by the approximate mean of Z. When $\hat{m}_Z^{(1)}$ is large, $\hat{R}_L$ can be approximated as

$$\tilde{R}_L = \hat{m}_Z^{(1)}. \quad (33)$$

The approximate upper bound of the average rate is given in Theorem 4.

Theorem 4: The approximate upper bound of R can be expressed as

$$\hat{R}_U = 9/8\ \hat{M}_Z\left(-1/3\right). \quad (34)$$

Proof: The proof can be found in Appendix A. ■

IV. NIG Approximation to Distribution of SINR in Logarithmic Domain

In this section, a brief description of the NIG distribution is given, and the distribution of the SINR in the logarithmic domain Z is approximated as the NIG distribution whose parameters are expressed in terms of the approximate mean, variance, skewness and kurtosis of Z. The expression for the CDF of the SINR based on the NIG approximation is also presented.

A. NIG Distribution

In the field of finance, the NIG approximation is introduced in [30], [34] where the four parameters of the NIG distribution are computed explicitly through the first four cumulants (mean, variance, skewness and kurtosis) of the target RV. In [34], numerical results show the NIG approximation performs better than the Gram-Charlier expansion [35] and Edgeworth expansion [36]. The expression for the NIG distribution [30], [34] is given by

$$f(z) = \frac{\alpha\delta}{\pi}\exp\left(\delta\sqrt{\alpha^2-\beta^2}-\beta\mu\right) \cdot \frac{K_1\left(\alpha\sqrt{\delta^2+(z-\mu)^2}\right)}{\sqrt{\delta^2+(z-\mu)^2}}\exp(\beta z),$$

where $K_1(\cdot)$ represents the modified Bessel function of the second kind with index 1, α, β, μ and δ are the tail heaviness parameter, asymmetry parameter, location parameter and scale parameter, respectively.

B. Computation of NIG Parameters

The approximate first four cumulants of the SINR in the logarithmic domain Z are given in Theorem 5.

Theorem 5: When the SF RVs X_i $(i = 0, \ldots, L)$ are independent from each other, the approximate first four cumulants of Z can be expressed as

$$\hat{c}_Z^{(1)} = \xi\mu_0 - \hat{m}_{Z_2}^{(1)}, \tag{35a}$$

$$\hat{c}_Z^{(2)} = (\xi\sigma_0)^2 + \hat{m}_{Z_2}^{(2)} - \left(\hat{m}_{Z_2}^{(1)}\right)^2, \tag{35b}$$

$$\hat{c}_Z^{(3)} = -\left[\hat{m}_{Z_2}^{(3)} - 3\hat{m}_{Z_2}^{(2)}\hat{m}_{Z_2}^{(1)} + 2\left(\hat{m}_{Z_2}^{(1)}\right)^3\right], \tag{35c}$$

$$\hat{c}_Z^{(4)} = \hat{m}_{Z_2}^{(4)} - 4\hat{m}_{Z_2}^{(3)}\hat{m}_{Z_2}^{(1)} - 3\left(\hat{m}_{Z_2}^{(2)}\right)^2 + 12\hat{m}_{Z_2}^{(2)}\left(\hat{m}_{Z_2}^{(1)}\right)^2 - 6\left(\hat{m}_{Z_2}^{(1)}\right)^4, \tag{35d}$$

respectively, where

$$\hat{m}_{Z_2}^{(n)} = \left(\frac{1}{\sqrt{\pi}}\right)^L \sum_{n_1=1}^{N_1}\cdots\sum_{n_L=1}^{N_L}\left(\prod_{i=1}^{L}\omega_{n_i}\right) \cdot\left\{\ln\left[\sum_{i=1}^{L}\kappa_{n_i}\left(a_{n_i};\mu_i,\sigma_i\right)+N_b\right]\right\}^n. \tag{36}$$

In interference-limited networks, when X_i $(i = 0, \ldots, L)$ are correlated and X_i $(i = 1, \ldots, L)$ have the same standard deviation σ_IdB, the approximate first four cumulants of Z can be given by

$$\hat{c}_Z^{(1)} = -\eta\ln r - \hat{m}_{Z_2'}^{(1)}, \tag{37a}$$

$$\hat{c}_Z^{(2)} = \xi^2\left(\sigma_0^2 - 2\zeta\sigma_0\sigma_I + \zeta\sigma_I^2\right) + \hat{m}_{Z_2'}^{(2)} - \left(\hat{m}_{Z_2'}^{(1)}\right)^2, \tag{37b}$$

$$\hat{c}_Z^{(3)} = -\left[\hat{m}_{Z_2'}^{(3)} - 3\hat{m}_{Z_2'}^{(2)}\hat{m}_{Z_2'}^{(1)} + 2\left(\hat{m}_{Z_2'}^{(1)}\right)^3\right], \tag{37c}$$

$$\hat{c}_Z^{(4)} = \hat{m}_{Z_2'}^{(4)} - 4\hat{m}_{Z_2'}^{(3)}\hat{m}_{Z_2'}^{(1)} - 3\left(\hat{m}_{Z_2'}^{(2)}\right)^2 + 12\hat{m}_{Z_2'}^{(2)}\left(\hat{m}_{Z_2'}^{(1)}\right)^2 - 6\left(\hat{m}_{Z_2'}^{(1)}\right)^4, \tag{37d}$$

respectively, where

$$\hat{m}_{Z_2'}^{(n)} = \left(\frac{1}{\sqrt{\pi}}\right)^L \sum_{n_1=1}^{N_1}\cdots\sum_{n_L=1}^{N_L}\left(\prod_{i=1}^{L}\omega_{n_i}\right) \cdot\left\{\ln\left[\sum_{i=1}^{L}\kappa_{n_i}\left(a_{n_i};-10\eta\lg d_i,\sigma_I\sqrt{1-\zeta}\right)\right]\right\}^n. \tag{38}$$

Proof: When X_i $(i = 0, \ldots, L)$ are independent from each other, with the MGF $\hat{M}_{Z_2}(s)$ of Z_2 in Theorem 1, the n-th order original moment of Z_2 can be presented as

$$\begin{aligned}\hat{m}_{Z_2}^{(n)} &= (-1)^n\frac{d^n\hat{M}_{Z_2}(s)}{ds^n}\Big|_{s=0} \\ &= \left(\frac{1}{\sqrt{\pi}}\right)^L \sum_{n_1=1}^{N_1}\cdots\sum_{n_L=1}^{N_L}\left(\prod_{i=1}^{L}\omega_{n_i}\right) \cdot\left\{\ln\left[\sum_{i=1}^{L}\kappa_{n_i}\left(a_{n_i};\mu_i,\sigma_i\right)+N_b\right]\right\}^n.\end{aligned} \tag{39}$$

Based on the relationship [31] between original moments and cumulants, the approximate first four cumulants of Z_2 can be computed through (39). With Lemma 1, the approximate first four cumulants of Z can be obtained.

In interference-limited networks, when X_i $(i = 0, \ldots, L)$ are correlated and X_i $(i = 1, \ldots, L)$ have the same standard deviation σ_IdB, with the MGF $\hat{M}_{Z_2'}(s)$ of Z_2' in Theorem 2, the n-th order original moment of Z_2' can be obtained from

$$\begin{aligned}\hat{m}_{Z_2'}^{(n)} &= (-1)^n\frac{d^n\hat{M}_{Z_2'}(s)}{ds^n}\Big|_{s=0} \\ &= \left(\frac{1}{\sqrt{\pi}}\right)^L \sum_{n_1=1}^{N_1}\cdots\sum_{n_L=1}^{N_L}\left(\prod_{i=1}^{L}\omega_{n_i}\right) \cdot\left\{\ln\left[\sum_{i=1}^{L}\kappa_{n_i}\left(a_{n_i};-10\eta\lg d_i,\sigma_I\sqrt{1-\zeta}\right)\right]\right\}^n.\end{aligned} \tag{40}$$

The approximate first four cumulants of Z_2' can be computed through (40). With Lemma 2, the approximate first four cumulants of Z can be obtained. ■

The approximate mean, variance, skewness and kurtosis of Z can be expressed as

$$\hat{m} = \hat{c}_Z^{(1)},\ \hat{v} = \hat{c}_Z^{(2)},\ \hat{s} = \frac{\hat{c}_Z^{(3)}}{\left(\hat{c}_Z^{(2)}\right)^{3/2}},\ \hat{k} = \frac{\hat{c}_Z^{(4)}}{\left(\hat{c}_Z^{(2)}\right)^2}, \tag{41}$$

respectively. According to [30], the four estimated parameters of the NIG distribution can be obtained from

$$\hat{\alpha} = 3\rho^{1/2}\,(\rho-1)^{-1}\,\hat{v}^{-1/2}\,\left|\hat{s}\right|^{-1}, \tag{42a}$$

$$\hat{\beta} = 3\,(\rho-1)^{-1}\,\hat{v}^{-1/2}\,\hat{s}^{-1}, \tag{42b}$$

$$\hat{\mu} = \hat{m} - 3\rho^{-1}\hat{v}^{1/2}\,\hat{s}^{-1}, \tag{42c}$$

$$\hat{\delta} = 3\rho^{-1}\,(\rho-1)^{1/2}\,\hat{v}^{1/2}\,\left|\hat{s}\right|^{-1}, \tag{42d}$$

where $\rho = 3\hat{k}\hat{s}^{-2} - 4$. To guarantee the feasibility of the NIG approximation, the following restriction condition [34] should be satisfied

$$\rho > 1.$$

Simulation results in Section V verify that this condition is satisfied in cellular networks with the system parameters defined in [11], although the rigorous mathematical proof remains an open problem and deserves a further investigation.

With the approximate distribution of Z, the approximate distribution of the SINR $Y = e^Z$ and rate $V = \ln\left(1+e^Z\right)$ can be expressed as

$$\hat{f}_Y(y) = \frac{CK_1\left(\hat{\alpha}\sqrt{\hat{\delta}^2 + \left(\ln y - \hat{\mu}\right)^2}\right)}{y\sqrt{\hat{\delta}^2 + \left(\ln y - \hat{\mu}\right)^2}}\exp\left(\hat{\beta}\ln y\right), \tag{43}$$

$$\hat{f}_V(v) = \frac{CK_1\left(\hat{\alpha}\sqrt{\hat{\delta}^2 + \left[\ln\left(\exp(v)-1\right) - \hat{\mu}\right]^2}\right)}{\left[\exp(v)-1\right]\sqrt{\hat{\delta}^2 + \left[\ln\left(\exp(v)-1\right) - \hat{\mu}\right]^2}} \cdot \exp\left[\hat{\beta}\ln\left(\exp(v)-1\right) + v\right], \tag{44}$$

respectively, where

$$C = \frac{\hat{\alpha}\hat{\delta}}{\pi}\exp\left(\hat{\delta}\sqrt{\hat{\alpha}^2 - \hat{\beta}^2} - \hat{\beta}\hat{\mu}\right). \tag{45}$$

C. CDF of SINR Based on NIG Approximation

As $P(Y \le y) = P(Z = \ln Y \le \ln y = z)$, the CDF of the SINR can be derived in the logarithmic domain.

Lemma 3: The CDF of the SINR based on the NIG approximation can be expressed as

$$\hat{F}(t) = \int_0^{+\infty} f_X(x)\,\Phi\left(\frac{t-\hat{\mu}-\hat{\beta}x}{\sqrt{x}}\right)dx, \tag{46}$$

where $\Phi(\cdot)$ is the CDF of the standard normal distribution.

Proof: According to [30], [34], if Z follows the NIG distribution with the parameters $\hat{\alpha}$, $\hat{\beta}$, $\hat{\mu}$ and $\hat{\delta}$, there exists a RV X that has the inverse Gaussian distribution [37] with the parameters $\hat{\delta}$ and $\gamma = \sqrt{\hat{\alpha}^2 - \hat{\beta}^2}$, and Z conditioned on X is normally distributed with the mean $\hat{\mu} + \hat{\beta}X$ and variance X. Thus the approximate distribution of Z based on the NIG distribution can be rewritten as

$$\hat{f}_Z(z) = \int_0^{+\infty} f_X(x)\,f_{Z|X}(z|x)\,dx, \tag{47}$$

where

$$f_X(x) = \frac{\hat{\delta}}{\sqrt{2\pi}}x^{-3/2}\exp\left(\hat{\delta}\gamma - \frac{\hat{\delta}^2}{2}x^{-1} - \frac{\gamma^2}{2}x\right),\ x>0, \tag{48a}$$

$$f_{Z|X}(z|x) = \frac{1}{\sqrt{2\pi x}}\exp\left[-\frac{\left(z-\hat{\mu}-\hat{\beta}x\right)^2}{2x}\right]. \tag{48b}$$

The CDF of Z can be given by

$$\begin{aligned}\hat{F}(t) &= \int_{-\infty}^{t}\int_0^{+\infty} f_{Z|X}(z|x)\,f_X(x)\,dxdz \\ &= \int_0^{+\infty} f_X(x)\int_{-\infty}^{t} f_{Z|X}(z|x)\,dzdx \\ &= \int_0^{+\infty} f_X(x)\,\Phi\left(\frac{t-\hat{\mu}-\hat{\beta}x}{\sqrt{x}}\right)dx.\end{aligned} \tag{49}$$

■

In the remaining part of this subsection, the approximation of the complementary error function erfc (x) is presented to obtain the closed-form expression for (46).

The complementary error function erfc (x) can be approximated as [38]

$$\text{erfc}(x) \approx \begin{cases} \sum_{k=1}^{M} a_k e^{-b_k x^2}, & x \ge 0, \\ 2 - \sum_{k=1}^{M} a_k e^{-b_k x^2}, & x < 0, \end{cases} \tag{50}$$

where $b_k = kb$, a_k and b are the coefficients of the approximation, and M is the order of the approximation. For $M = 6, 7, 8, 9$, the coefficients are shown in Table I where both the root mean square error (RMSE) and adjusted R-square [39] are used to evaluate the performance of the approximation. It can be seen that when M is no less than 8, the approximation can get the satisfactory performance. Substituting (50) into the identity

$$\Phi(x) = 1 - \frac{1}{2}\text{erfc}\left(\frac{x}{\sqrt{2}}\right),$$

the approximation of $\Phi(x)$ can be written as

$$\Phi(x) \approx \begin{cases} 1 - \frac{1}{2}\sum_{k=1}^{M} a_k \exp\left(-\frac{b_k}{2}x^2\right), & x \ge 0, \\ \frac{1}{2}\sum_{k=1}^{M} a_k \exp\left(-\frac{b_k}{2}x^2\right), & x < 0. \end{cases} \tag{51}$$

Simulation results in Section V verify that the SINR in the logarithmic domain Z is negatively skewed in cellular networks with the system parameters defined in [11], the corresponding mathematical proof, however, requires a further study. When the skewness of Z is negative, $\hat{\beta}$ is less than 0. In this case, the closed-form approximation for $\hat{F}(t)$ is given in Theorem 6.

TABLE I
APPROXIMATION OF erfc (x)

Order	$[a_k], k = 1, \ldots, M$	b	RMSE	Adjust R-square
6	[0.9188, −0.6471, −3.895, 17.38, −23.01, 10.22]	1.51	9.93×10^{-4}	0.9997
7	[1.56, −10.46, 57.21, −163.3, 249.1, −191.7, 58.55]	1.636	7.06×10^{-4}	0.9998
8	[1.109, −2.958, −1.231, 67.68, −249.8, 405.8, −313.9, 94.25]	1.524	6.64×10^{-4}	0.9999
9	[1.706, −18.29, 163.8, −816.1, 2384, −4174, 4303, −2406, 562.5]	1.614	5.12×10^{-4}	0.9999

Theorem 6: $\hat{F}(t)$ can be approximated as

$$\tilde{F}(t) = \begin{cases} 1 - \frac{1}{2}\hat{\delta}\exp\left(\hat{\delta}\gamma\right) \\ \quad \cdot \sum_{k=1}^{M} \frac{a_k}{A_k}\exp\left(b_k\hat{\beta}^2 q - A_k B_k\right), & t \geq \hat{\mu}, \\ \frac{1}{2}\left[1 + \operatorname{erf}(V_2)\right] - \frac{1}{2}\exp\left(2\hat{\delta}\gamma\right)\operatorname{erfc}(V_1) \\ \quad + \frac{1}{2}\hat{\delta}\exp\left(\hat{\delta}\gamma\right)\sum_{k=1}^{M}\frac{a_k}{A_k}\exp\left(q\hat{\beta}^2 b_k\right) \\ \quad \cdot \left[\exp(A_k B_k)\operatorname{erfc}(C_k) \right. \\ \quad \left. - \exp(-A_k B_k)\operatorname{erf}(D_k)\right], & t < \hat{\mu}. \end{cases}$$

where

$$q = \frac{t - \hat{\mu}}{\hat{\beta}}, \tag{52a}$$

$$A_k = \sqrt{\hat{\delta}^2 + q^2\hat{\beta}^2 b_k}, \quad B_k = \sqrt{\gamma^2 + \hat{\beta}^2 b_k}, \tag{52b}$$

$$V_1 = \frac{\hat{\delta}}{\sqrt{2q}} + \gamma\sqrt{\frac{q}{2}}, \quad V_2 = \frac{\hat{\delta}}{\sqrt{2q}} - \gamma\sqrt{\frac{q}{2}}, \tag{52c}$$

$$C_k = \frac{A_k}{\sqrt{2q}} + B_k\sqrt{\frac{q}{2}}, \; D_k = \frac{A_k}{\sqrt{2q}} - B_k\sqrt{\frac{q}{2}}. \tag{52d}$$

Proof: The proof can be found in Appendix B. ■

V. NUMERICAL RESULTS

In this section, the performance of the lower and upper bounds of the average rate, restriction condition of the NIG approximation, skewness of the SINR in the logarithmic domain and performance of the NIG approximation are investigated for cellular networks whose system parameters [11] are given in Table II. Numerical computations and Monte Carlo simulations are performed to verify the derivation and show the impacts of the UE location, ISD, path loss exponent, SF correlation coefficient and standard deviation of the SF.

A. Lower and Upper Bounds of Average Rate

In this subsection, the performance of the lower and upper bounds of the average rate is investigated for UE1, UE2 and UE3. The ISD is 1732m, and the Monte Carlo simulation with 5000000 trials is conducted for comparison. The results versus the standard deviation of the SF are depicted in Fig. 2(a). The SF RVs X_i $(i = 0, \ldots, L)$ are independent and have the same standard deviation, and the path loss exponent is 3.76. It can be seen that the lower bound almost coincides with the Monte Carlo simulation for the UEs near to the BS. And the performance of the approximate mean of the SINR in the logarithmic domain Z is similar to that of the lower bound for these UEs. For the UEs at the cell edge and in the middle of the cell, both the lower and upper bound are quite tight.

TABLE II
SETTING OF SYSTEM PARAMETERS

System parameter	Parameter value
ISD	100m, 500m, 1732m or 2000m
Number of interfering cells	6
Path loss constant	15.3dB
Transmit power of BS	46dBm
BS antenna gain after cable loss	14dBi
Minimum distance between the UE and BS	35m
Path loss exponent	2∼4
UE noise figure	9dB
Ambient temperature	300K
Standard deviation of the SF	4∼10dB
SF correlation coefficient	0.1∼0.8
Order of the approximation of erfc (x)	8
UE locations	UE1: $(4/5\ D, \pi/5)$ UE2: $(1/2\ D, \pi/5)$ UE3: $(1/5\ D, \pi/5)$

Fig. 2(b) depicts the performance of the lower and upper bounds versus the path loss exponent. X_i $(i = 0, \ldots, L)$ are independent and the standard deviations of them are 8dB. For the UEs near to the BS, the lower bound almost coincides with the Monte Carlo simulation, and the performance of the approximate mean of Z is similar to that of the lower bound. Both the lower and upper bound are quite tight for the UEs at the cell edge and in the middle of the cell. With the system parameters in Table II, cellular networks are interference-limited, thus the background noise can be ignored compared to the inter-cell interference. As the distance d_i $(i = 1, \ldots, L)$ between the UE and BS of the i-th interfering cell is larger than the distance r between the UE and BS of the serving cell, the total inter-cell interference decreases more quickly than the useful signal when the path loss exponent increases. Thus the SINR increases with path loss exponent, makes the average rate also increase with path loss exponent, as shown in Fig. 2(b).

The performance of the lower and upper bounds versus the SF correlation coefficient is shown in Fig. 2(c). The standard deviations of the SF RVs are 8dB and the path loss exponent is 3.76. It can be found that the lower bound almost coincides with the Monte Carlo simulation for the UEs near to the BS. And the performance of the approximate mean of Z is similar to that of the lower bound for these UEs. The bounds are quite tight for the UEs at the cell edge and in the middle of the cell. As is indicated in Lemma 2, when the standard deviation of X_0 is the same as that of X_i $(i = 1, ..., L)$, the impact of the SF correlation coefficient on the average rate and its lower and upper bounds is opposite to that of the standard deviation of the SF.

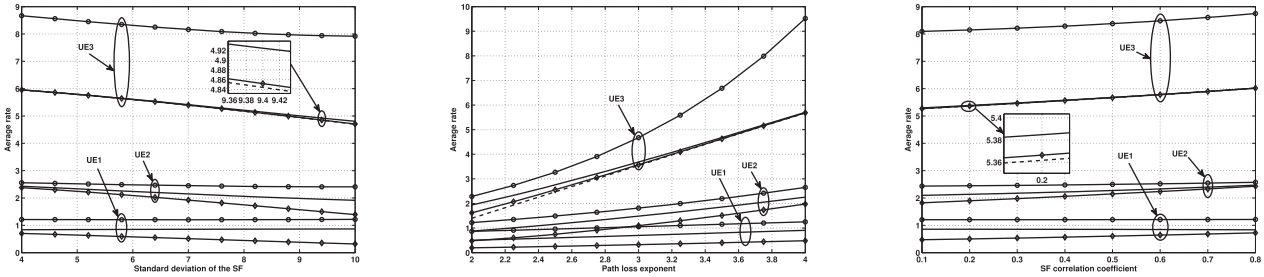

(a) Bounds of the average rate versus the standard deviation of the SF. (b) Bounds of the average rate versus the path loss exponent. (c) Bounds of the average rate versus the SF correlation coefficient.

Fig. 2. Lower and upper bounds of the average rate. Solid lines without marks denote the Monte simulation. Solid lines marked with diamonds and circles represent the lower and upper bound, respectively. Dashed lines stand for the approximate mean of the SINR in the logarithmic domain.

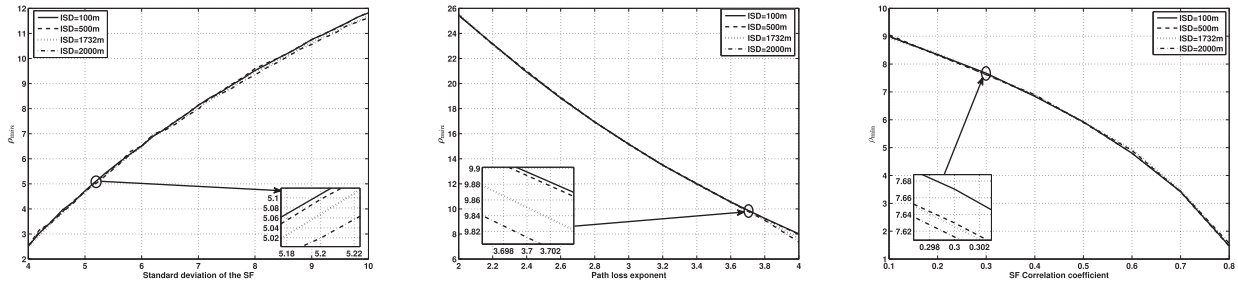

(a) ρ_{min} in terms of the standard deviation of the (b) ρ_{min} in terms of the path loss exponent. (c) ρ_{min} in terms of the SF correlation coefficient.

Fig. 3. Variation of ρ_{min}.

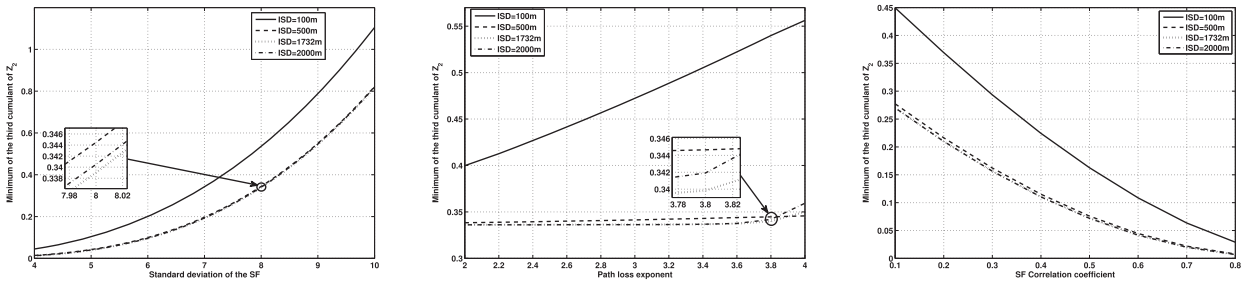

(a) $\left(\hat{c}_{Z_2}^{(3)}\right)_{min}$ versus the standard deviation of the SF. (b) $\left(\hat{c}_{Z_2}^{(3)}\right)_{min}$ versus the path loss exponent. (c) $\left(\hat{c}_{Z_2}^{(3)}\right)_{min}$ versus the SF correlation coefficient.

Fig. 4. Variation of $\left(\hat{c}_{Z_2}^{(3)}\right)_{min}$.

B. Restriction Condition of NIG Approximation

The restriction condition $\rho > 1$ of the NIG approximation is verified in this subsection. The calculations of ρ are conducted for 10000 UEs uniformly distributed within the serving cell, and the minimum of them ρ_{min} is shown in Fig. 3(a), Fig. 3(b), and Fig. 3(c) in terms of the standard deviation of the SF, path loss exponent and SF correlation coefficient, respectively. In Fig. 3(a), the SF RVs are independent and have the same standard deviation, and the path loss exponent is 3.76. It can be seen that ρ_{min} is larger than 1 for different ISDs, and ρ_{min} changes little with ISD. In Fig. 3(b), the SF RVs are independent and the standard deviations of them are 8dB. It is shown that the restriction condition of the NIG distribution is satisfied for different ISDs, and the ISD also has little impact on ρ_{min}. The standard deviations of the SF RVs are 8dB and the path loss exponent is 3.76 in Fig. 3(c). It can be observed that ρ_{min} is more than 1 for different ISDs, and ρ_{min} does not change much with ISD. Therefore, the distribution of the SINR in the logarithmic domain for any UE in the serving cell is allowable to be approximated as the NIG distribution, and the ISD has little impact on ρ_{min}.

C. Skewness of SINR in Logarithmic Domain

In this subsection, it is verified that the skewness of the SINR in the logarithmic domain Z is negative in cellular networks. The computations of the approximate third cumulant $\hat{c}_{Z_2}^{(3)}$ of the interference plus noise in the logarithmic domain Z_2 are conducted for 10000 UEs uniformly distributed in the serving cell, and the minimum of them $\left(\hat{c}_{Z_2}^{(3)}\right)_{min}$ is depicted in Fig. 4(a), Fig. 4(b) and Fig. 4(c) versus the standard deviation of the SF, path loss exponent and SF correlation coefficient,

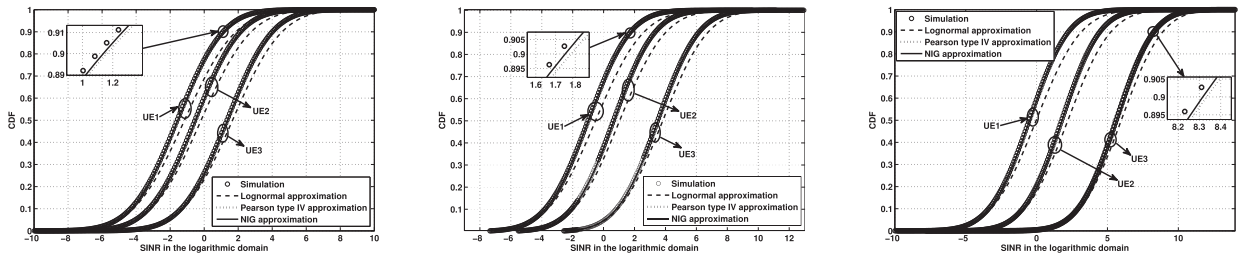

(a) Case I. (b) Case II. (c) Case III.

Fig. 5. CDFs of the Monte Carlo simulation, lognormal approximation and NIG approximation for cases I∼III. The data in the horizontal axis denote the values of Z.

respectively. In Fig. 4(a), the SF RVs are independent and have the same standard deviation, and the path loss exponent is 3.76. It can be found that $\left(\hat{c}_{Z_2}^{(3)}\right)_{min}$ is positive for different ISDs. Moreover, $\left(\hat{c}_{Z_2}^{(3)}\right)_{min}$ increases with standard deviation of the SF. Considering the fact that the third cumulant of the Gaussian RV is zero, the distribution of Z_2 deviates more from the Gaussian distribution with the increase of standard deviation of the SF. Therefore it is not feasible to assume Z to be a Gaussian RV when the standard deviations of the SF are large. In Fig. 4(b),the SF RVs are independent and the standard deviations of them are 8dB. It can be observed that $\left(\hat{c}_{Z_2}^{(3)}\right)_{min}$ is larger than zero for different ISDs. The standard deviations of the SF RVs are 8dB and the path loss exponent is 3.76 in Fig. 4(c). It is shown that $\left(\hat{c}_{Z_2}^{(3)}\right)_{min}$ is more than zero for different ISDs. Moreover, $\left(\hat{c}_{Z_2}^{(3)}\right)_{min}$ decrease with SF correlation coefficient. Thus Z is more likely to be a Gaussian RV when the SF correlation coefficient is large. In summary, the third cumulant of Z_2 is positive for any UE in the cell range. As the third cumulant of Z is the opposite of that of Z_2, the skewness of Z is negative.

D. Performance of NIG Approximation

The performances of the lognormal approximation, Pearson type IV approximation [23] and NIG approximation are compared in this subsection. The ISD is 1732m, and the Monte Carlo simulation with 5000000 trials is conducted for comparison. The start point of computing the parameters of the MGF-based lognormal approximation [17], [26] to the inter-cell interference plus noise is specified by the Wilkinson's method [40]. The RMSE performances of the CDF $\hat{F}(t)$ of the SINR based on the NIG approximation and approximate CDF $\tilde{F}(t)$ derived in this paper are also presented. When the SF RVs are independent, the following seven cases are examined.

- Case I, $\eta = 2, \sigma_0 = \sigma_1 = \ldots = \sigma_L = 8$dB.
- Case II, $\eta = 3, \sigma_0 = \sigma_1 = \ldots = \sigma_L = 8$dB.
- Case III, $\eta = 4, \sigma_0 = \sigma_1 = \ldots = \sigma_L = 8$dB.
- Case IV, $\sigma_0 = \sigma_1 = \ldots = \sigma_L = 4$dB, $\eta = 3.76$.
- Case V, $\sigma_0 = \sigma_1 = \ldots = \sigma_L = 8$dB, $\eta = 3.76$.
- Case VI, $\sigma_0 = \sigma_1 = \ldots = \sigma_L = 12$dB, $\eta = 3.76$.
- Case VII, $\sigma_0 = \sigma_1 = 8$dB, $\sigma_2 = 4$dB, $\sigma_3 = 6$dB, $\sigma_4 = 7$dB and $\sigma_5 = \sigma_6 = 10$dB, $\eta = 3.76$.

Cases I∼III take the variation of the path loss exponent into account, while cases IV∼VII consider the variation of the standard deviation of the SF.

The results for cases I∼III are shown in Fig. 5. The lognormal approximation does not work well for different UE locations, while the Pearson type IV approximation and NIG approximation can always get the satisfactory performance. Fig. 6 depicts the results for cases IV∼VII. The Pearson type IV approximation and NIG approximation can always get the satisfactory performance. The performance of the lognormal approximation is similar to that of the Pearson type IV approximation and NIG approximation when the standard deviations of the SF are small. When the standard deviations of the SF are large, the lognormal approximation significantly deviates from the Monte Carlo simulation. This is in accordance with the results in Fig. 4(a). The performance of the lognormal approximation is also poor when the standard deviations of the SF are different.

To illustrate the impact of the SF correlation coefficient, the following two cases are investigated:

- Case VIII, $\sigma_0 = \sigma_1 = \ldots = \sigma_6 = 8$dB, $\eta = 3.76$, $\zeta = 0.2$.
- Case IX, $\sigma_0 = \sigma_1 = \ldots = \sigma_6 = 8$dB, $\eta = 3.76$, $\zeta = 0.6$.

The results are depicted in Fig. 7. The Pearson type IV approximation and NIG approximation can get the better performance than the lognormal approximation when the SF correlation coefficient is small. When the SF correlation coefficient is large, the performance of the lognormal approximation becomes better. This is in accordance with the results in Fig. 4(c).

The Kullback–Leibler divergence [41] of the lognormal approximation, Pearson type IV approximation and NIG approximation from the Monte Carlo simulation for UE1, UE2 and UE3 is presented in Table III, IV and V, respectively. The performance of the lognormal approximation is sensitive to the standard deviation of the SF, while the performances of the Pearson type IV approximation and NIG approximation are robust to the UE location, path loss exponent, SF correlation coefficient and standard deviation of the SF. The superiority of the NIG approximation over the Pearson type IV approximation can be found from the Kullback–Leibler divergence performance. The NIG approximation is more accurate than the Pearson type IV approximation, and the performance of the NIG approximation is more robust to the UE location, path loss exponent, SF correlation coefficient and standard

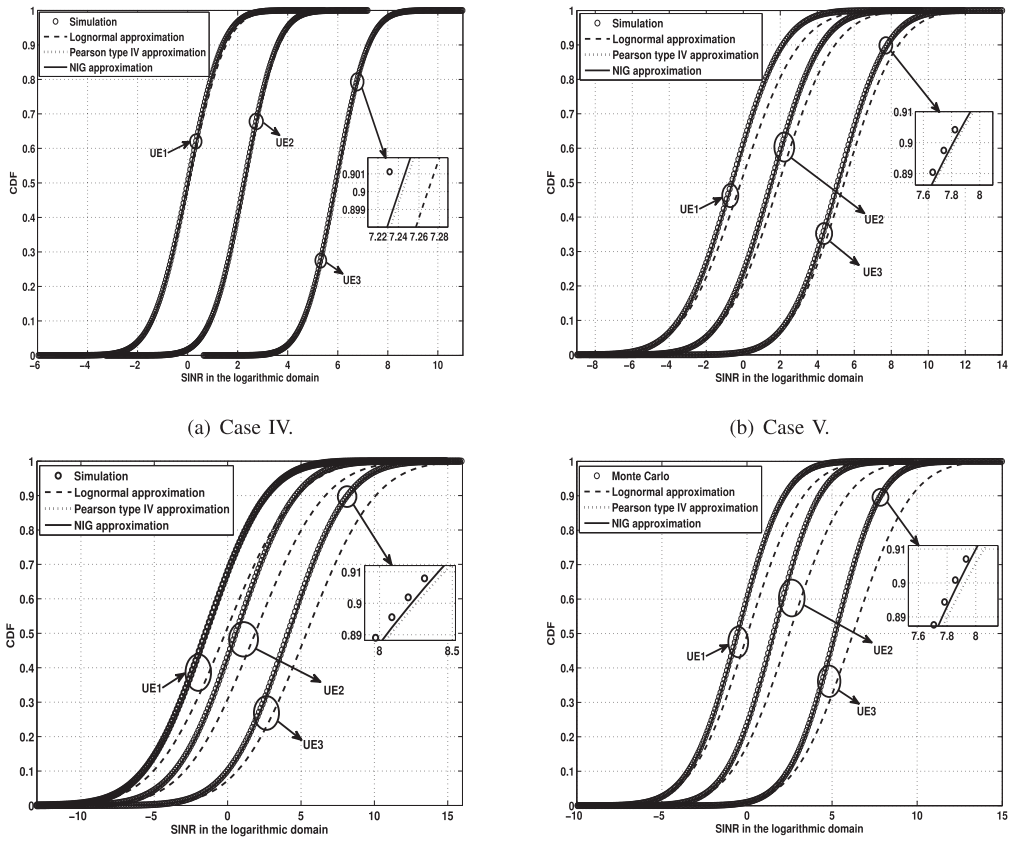

(a) Case IV. (b) Case V.

(c) Case VI. (d) Case VII.

Fig. 6. CDFs of the Monte Carlo simulation, lognormal approximation and NIG approximation for cases IV∼VII. The data in the horizontal axis represent the values of Z.

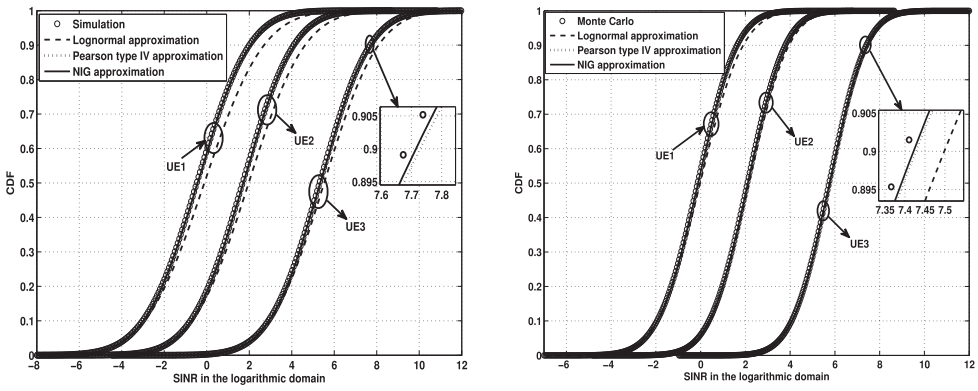

(a) Case VIII. (b) Case IX.

Fig. 7. CDFs of the Monte Carlo simulation, lognormal approximation and NIG approximation for cases VII∼IX. The data in the horizontal axis denote the values of Z.

deviation of the SF. When the SF correlation coefficient is small or the standard deviations of the SF are large or different, the NIG approximation is up to one order of magnitude more accurate than the Pearson type IV approximation and at least one order of magnitude more accurate than the lognormal approximation.

Table VI and VII present the RMSE between $\hat{F}(t)$ which is computed through numerical integration and the Monte Carlo simulation and RMSE between $\tilde{F}(t)$ and the Monte Carlo simulation, respectively. Numerical results show that the performance of $\tilde{F}(t)$ is robust to the UE location, path loss exponent, SF correlation coefficient and standard deviation of the SF. If the approximation is considered to be accurate when the RMSE is in the order of 0.001, the CDF of the SINR can be well approximated as (52) that is more tractable than the numerical computation and Monte Carlo simulation.

TABLE III
KULLBACK–LEIBLER DIVERGENCE OF THE LOGNORMAL APPROXIMATION, PEARSON TYPE IV APPROXIMATION AND NIG APPROXIMATION FOR UE1

Cases	Lognormal	Pearson type IV	NIG
case I	2.90×10^{-2}	9.71×10^{-4}	2.03×10^{-4}
case II	3.56×10^{-2}	1.45×10^{-3}	1.86×10^{-4}
case III	3.72×10^{-2}	2.21×10^{-3}	2.08×10^{-4}
case IV	4.45×10^{-3}	1.76×10^{-3}	1.76×10^{-4}
case V	3.70×10^{-2}	1.99×10^{-3}	2.05×10^{-4}
case VI	8.65×10^{-2}	1.68×10^{-3}	1.80×10^{-4}
case VII	5.36×10^{-2}	3.97×10^{-3}	1.87×10^{-4}
case VIII	2.69×10^{-2}	1.95×10^{-3}	1.67×10^{-4}
case IX	9.32×10^{-3}	1.90×10^{-3}	1.81×10^{-4}

TABLE IV
KULLBACK–LEIBLER DIVERGENCE OF THE LOGNORMAL APPROXIMATION, PEARSON TYPE IV APPROXIMATION AND NIG APPROXIMATION FOR UE2

Cases	Lognormal	Pearson type IV	NIG
case I	2.13×10^{-2}	7.25×10^{-4}	2.00×10^{-4}
case II	2.51×10^{-2}	8.38×10^{-4}	1.78×10^{-4}
case III	3.01×10^{-2}	1.12×10^{-3}	1.91×10^{-4}
case IV	1.60×10^{-3}	5.72×10^{-4}	1.72×10^{-4}
case V	2.85×10^{-2}	1.03×10^{-3}	1.93×10^{-4}
case VI	8.60×10^{-2}	1.14×10^{-3}	1.69×10^{-4}
case VII	1.05×10^{-1}	3.50×10^{-3}	2.34×10^{-4}
case VIII	1.85×10^{-2}	9.70×10^{-4}	2.05×10^{-4}
case IX	4.04×10^{-3}	7.16×10^{-4}	1.80×10^{-4}

TABLE V
KULLBACK–LEIBLER DIVERGENCE OF THE LOGNORMAL APPROXIMATION, PEARSON TYPE IV APPROXIMATION AND NIG APPROXIMATION FOR UE3

Cases	Lognormal	Pearson type IV	NIG
case I	1.80×10^{-2}	6.28×10^{-4}	1.89×10^{-4}
case II	1.86×10^{-2}	6.14×10^{-4}	1.64×10^{-4}
case III	2.06×10^{-2}	7.45×10^{-4}	2.07×10^{-4}
case IV	5.28×10^{-4}	2.47×10^{-4}	1.67×10^{-4}
case V	1.97×10^{-2}	7.03×10^{-4}	2.08×10^{-4}
case VI	7.96×10^{-2}	9.65×10^{-4}	1.86×10^{-4}
case VII	1.29×10^{-1}	3.30×10^{-3}	1.76×10^{-4}
case VIII	1.09×10^{-2}	5.94×10^{-4}	1.92×10^{-4}
case IX	1.47×10^{-3}	3.48×10^{-4}	1.78×10^{-4}

TABLE VI
RMSE BETWEEN $\hat{F}(t)$ AND THE MONTE CARLO SIMULATION

Cases	UE1	UE2	UE3
case I	1.50×10^{-4}	1.15×10^{-4}	1.99×10^{-4}
case II	1.99×10^{-4}	1.13×10^{-4}	1.16×10^{-4}
case III	9.17×10^{-5}	2.13×10^{-4}	1.03×10^{-4}
case IV	1.29×10^{-4}	2.51×10^{-4}	1.50×10^{-4}
case V	1.41×10^{-4}	2.13×10^{-4}	1.34×10^{-4}
case VI	1.34×10^{-4}	2.13×10^{-4}	1.80×10^{-4}
case VII	1.23×10^{-4}	1.71×10^{-4}	1.44×10^{-4}
case VIII	7.36×10^{-5}	2.52×10^{-4}	2.04×10^{-4}
case IX	1.25×10^{-4}	1.65×10^{-4}	1.03×10^{-4}

TABLE VII
RMSE BETWEEN $\tilde{F}(t)$ AND THE MONTE CARLO SIMULATION

Cases	UE1	UE2	UE3
case I	9.59×10^{-4}	1.01×10^{-3}	1.03×10^{-3}
case II	8.71×10^{-4}	9.18×10^{-4}	1.00×10^{-3}
case III	7.17×10^{-4}	9.35×10^{-4}	9.65×10^{-4}
case IV	7.29×10^{-4}	1.07×10^{-3}	1.20×10^{-3}
case V	8.06×10^{-4}	9.53×10^{-4}	1.01×10^{-3}
case VI	7.77×10^{-4}	9.29×10^{-4}	9.20×10^{-4}
case VII	5.64×10^{-4}	7.36×10^{-4}	8.12×10^{-4}
case VIII	7.27×10^{-4}	9.60×10^{-4}	1.09×10^{-3}
case IX	7.24×10^{-4}	9.86×10^{-4}	1.16×10^{-3}

VI. CONCLUSIONS

For OFDMA-based cellular networks where the distance-dependent path loss and SF are considered, the closed-form approximation for the lower and upper bounds of the downlink average rate has been presented, and the distribution of the downlink SINR in the logarithmic domain has been proposed to be approximated as the NIG distribution. The lower bound of the average rate has been expressed in terms of the analytical approximate mean of the SINR in the logarithmic domain, and the upper bound of the average rate has been presented through the value of the analytical approximate MGF $\hat{M}_Z(s)$ of the SINR in the logarithmic domain Z at $s = -1/3$. The parameters of the NIG approximation have been computed explicitly through the closed-form approximation for the mean, variance, skewness and kurtosis of the SINR in the logarithmic domain. The closed-form expression for the CDF of the SINR based on the NIG approximation has also been obtained in terms of exponential functions and error functions. Simulation results have verified the tightness of the lower and upper bounds of the average rate. For the UEs near to the BS, the lower bound almost coincides with the Monte Carlo simulation, and the performance of the approximate mean of the SINR in the logarithmic domain is similar to that of the lower bound. For the UEs at the cell edge and in the middle of cell, both the lower and upper bound are quite tight. The feasibility and accuracy of the NIG approximation have also been verified through simulation results. Compared to the performances of the lognormal approximation and Pearson type IV approximation, the performance of the NIG approximation is more robust to the UE location, path loss exponent, SF correlation coefficient and standard deviation of the SF. When the SF correlation coefficient is large or the standard deviations of the SF are small, the lognormal approximation, Pearson type IV approximation and NIG approximation have the similar performance. When the SF correlation coefficient is small or the standard deviations of the SF are large or different, the NIG approximation is up to one order of magnitude more accurate than the Pearson type IV approximation and at least one order of magnitude more accurate than the lognormal approximation. Besides, it has been verified through simulation results that the closed-form expression for the CDF of the SINR based on the NIG approximation can always get the satisfactory performance.

APPENDIX A
PROOF OF THEOREM 4

To obtain the approximate upper bound of the average rate, the following inequality is proved at first:

$$\ln(1+x) \le 9/8\, x^{1/3},\ x \ge 0. \tag{53}$$

For $x = 0$, (53) is obvious. For $x > 0$, (53) is equivalent to

$$g(x) = \ln(1+x) - 9/8\, x^{1/3} \le 0,\ x > 0. \tag{54}$$

Next, the sign of the first derivative of $g(x)$ is analyzed to present the monotonicity of $g(x)$. Then the maximum value of $g(x)$ is solved to prove that $g(x)$ is negative in the range of $(0, +\infty)$.

The first derivative of $g(x)$ is

$$h(x) = \frac{1}{1+x} - 3/8\, x^{-2/3} = \frac{8x^{2/3} - 3(1+x)}{8(1+x)x^{2/3}}. \tag{55}$$

It can be seen that the denominator of $h(x)$ is positive. Let the numerator of $h(x)$ represented as $r(x) = 8x^{2/3} - 3(1+x)$. The first derivative of $r(x)$ is $u(x) = 16/3\, x^{-1/3} - 3$. As

$$u(x) > 0,\ x \in \left(0, \left(\frac{16}{9}\right)^3\right), \tag{56a}$$

$$u(x) = 0,\ x = \left(\frac{16}{9}\right)^3, \tag{56b}$$

$$u(x) < 0,\ x \in \left(\left(\frac{16}{9}\right)^3, +\infty\right), \tag{56c}$$

$r(x)$ monotonically increases when $x < \left(\frac{16}{9}\right)^3$, and monotonically decreases when $x > \left(\frac{16}{9}\right)^3$. Note that

$$r(x)|_{x\to 0+0} = -3 < 0, \tag{57a}$$

$$r\left(\left(\frac{16}{9}\right)^3\right) \approx 5.43 > 0, \tag{57b}$$

$$r(x)|_{x\to+\infty} = \lim_{x\to+\infty} \frac{8 - 3\left(x^{-2/3} + x^{1/3}\right)}{x^{-2/3}} = -\infty, \tag{57c}$$

thus there exist two zero points of $r(x)$ in the range of $(0, +\infty)$. Denote the smaller and larger zero point as e_1 and e_2, respectively. e_1 is in the range of $\left(0, \left(\frac{16}{9}\right)^3\right)$, and e_2 locates in the range of $\left(\left(\frac{16}{9}\right)^3, +\infty\right)$. Furthermore,

$$r(x) < 0,\ x \in (0, e_1) \text{ or } x \in (e_2, +\infty), \tag{58a}$$

$$r(x) > 0,\ e_1 < x < e_2. \tag{58b}$$

From the above analysis, the curve of $r(x)$ can be intuitively plotted in Fig. 8. The sign of $h(x)$ is the same with that of $r(x)$, therefore

$$g(x) < g(0) = 0,\ x \in (0, e_1), \tag{59a}$$

$$g(x) \le g(e_2),\quad x \in [e_1, e_2], \tag{59b}$$

$$g(x) < g(e_2),\quad x \in (e_2, +\infty). \tag{59c}$$

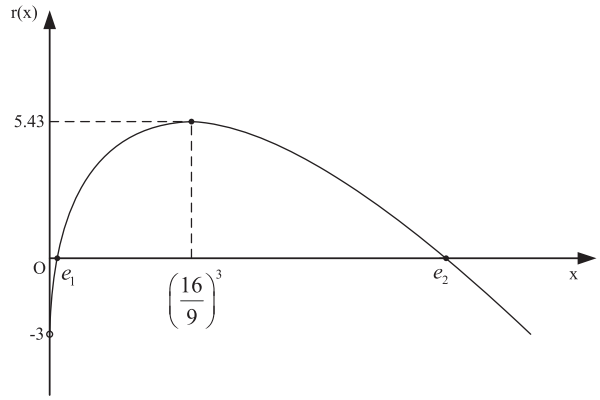

Fig. 8. Intuitive curve of $r(x)$.

The zeros of $r(x)$ can be obtained by solving the equation

$$8x^{2/3} - 3(1+x) = 0. \tag{60}$$

Taking the substitution $t = x^{\frac{1}{3}} > 0$, (60) can be rewritten as

$$3t^3 - 8t^2 + 3 = 0. \tag{61}$$

Using the Shengjin's formula [42], the two positive solutions of (61) can be given by

$$t_1 = \frac{8 + 8\left[\cos\frac{\arccos(-295/1024)}{3} - \sqrt{3}\sin\frac{\arccos(-295/1024)}{3}\right]}{9}, \tag{62a}$$

$$t_2 = \frac{8 + 8\left[\cos\frac{\arccos(-295/1024)}{3} + \sqrt{3}\sin\frac{\arccos(-295/1024)}{3}\right]}{9}. \tag{62b}$$

Then

$$e_1 = t_1^3 \approx 0.367048,\ e_2 = t_2^3 \approx 15.768691. \tag{63}$$

With the value of e_2 in (63), the value of $g(x)$ at e_2 can be presented as $g(e_2) \approx -0.001582 < 0$. Thus $g(x)$ is negative in the range of $(0, +\infty)$.

With the inequality (53), the upper bound of the average rate can be given by

$$R \le R_U = E\left[9/8\, e^{1/3\, Z}\right] = 9/8\ M_Z(s)|_{s=-1/3}. \tag{64}$$

Replacing the MGF $M_Z(s)$ of Z with its approximation $\hat{M}_Z(s)$, (34) can be obtained.

APPENDIX B
PROOF OF THEOREM 6

Based on (51), (46) can be approximated as

$$\tilde{F}(t) = \int_{x\in\mathcal{A}} f_X(x)\left\{1 - \frac{1}{2}\sum_{k=1}^{M} a_k \exp\left[-\frac{b_k t_x^2}{2x}\right]\right\}dx + \int_{x\in\mathcal{B}} f_X(x)\left\{\frac{1}{2}\sum_{k=1}^{M} a_k \exp\left[-\frac{b_k t_x^2}{2x}\right]\right\}dx, \tag{65}$$

where

$$t_x = t - \hat{\mu} - \hat{\beta}x \tag{66a}$$

$$\mathcal{A} = \{x : t_x \geq 0\} \cap (0, +\infty), \ \mathcal{B} = \{x : t_x < 0\} \cap (0, +\infty). \tag{66b}$$

When t is no less than $\hat{\mu}$, t_x is positive for any $x \in (0, +\infty)$, thus $\tilde{F}(t)$ can be rewritten as

$$\begin{aligned}\tilde{F}(t) &= \int_0^{+\infty} f_X(x) \left[1 - \frac{1}{2}\sum_{k=1}^{M} a_k \exp\left(-\frac{b_k t_x^2}{2x}\right)\right] dx \\ &= 1 - E_2,\end{aligned} \tag{67}$$

where

$$E_2 = \frac{1}{2}\frac{\hat{\delta}}{\sqrt{2\pi}} \exp\left(\hat{\delta}\gamma\right) \sum_{k=1}^{M} a_k \exp\left(b_k \hat{\beta}^2 q\right) E_{2,k}, \tag{68a}$$

$$E_{2,k} = \int_0^{+\infty} x^{-3/2} \exp\left(-\frac{A_k^2}{2}x^{-1} - \frac{B_k^2}{2}x\right) dx. \tag{68b}$$

Take the substitution $u = x^{-1/2}$, then $E_{2,k}$ can be rewritten as

$$\begin{aligned}E_{2,k} &= 2\int_0^{+\infty} \exp\left(-\frac{A_k^2}{2}u^2 - \frac{B_k^2}{2}u^{-2}\right) du \\ &= \frac{\sqrt{2\pi}}{A_k} \exp\left(-A_k B_k\right).\end{aligned} \tag{69}$$

The last equality follows from the formula [18]

$$\int_0^{+\infty} \exp\left(-ax^2 - bx^{-2}\right) dx = \frac{1}{2}\sqrt{\frac{\pi}{a}} \exp\left(-2\sqrt{ab}\right).$$

Thus

$$E_2 = \frac{1}{2}\hat{\delta} \exp\left(\hat{\delta}\gamma\right) \sum_{k=1}^{M} \frac{a_k}{A_k} \exp\left(q\hat{\beta}^2 b_k - A_k B_k\right). \tag{70}$$

When t is less than $\hat{\mu}$, t_x is positive for $x > q$, and negative for $x < q$, thus $\tilde{F}(t)$ can be rewritten as

$$\begin{aligned}\tilde{F}(t) = &\int_q^{+\infty} \frac{\hat{\delta}}{\sqrt{2\pi}} x^{-3/2} \exp\left(\hat{\delta}\gamma - \frac{\hat{\delta}^2}{2}x^{-1} - \frac{\gamma^2}{2}x\right) \\ &\cdot \left[1 - \frac{1}{2}\sum_{k=1}^{M} a_k \exp\left(-\frac{b_k t_x^2}{2x}\right)\right] dx \\ &+ \int_0^{q} \frac{\hat{\delta}}{\sqrt{2\pi}} x^{-3/2} \exp\left(\hat{\delta}\gamma - \frac{\hat{\delta}^2}{2}x^{-1} - \frac{\gamma^2}{2}x\right) \\ &\cdot \left[\frac{1}{2}\sum_{k=1}^{M} a_k \exp\left(-\frac{b_k t_x^2}{2x}\right)\right] dx = E_3 - E_4 + E_5,\end{aligned} \tag{71}$$

where

$$E_3 = \int_q^{+\infty} \frac{\hat{\delta}}{\sqrt{2\pi}} x^{-3/2} \exp\left(\hat{\delta}\gamma - \frac{\hat{\delta}^2}{2}x^{-1} - \frac{\gamma^2}{2}x\right) dx, \tag{72a}$$

$$E_4 = \frac{1}{2}\frac{\hat{\delta}}{\sqrt{2\pi}} \exp\left(\hat{\delta}\gamma\right) \sum_{k=1}^{M} a_k \exp\left(b_k \hat{\beta}^2 q\right) E_{4,k}, \tag{72b}$$

$$E_{4,k} = \int_q^{+\infty} x^{-3/2} \exp\left(-\frac{A_k^2}{2}x^{-1} - \frac{B_k^2}{2}x\right) dx, \tag{72c}$$

$$E_5 = \frac{1}{2}\frac{\hat{\delta}}{\sqrt{2\pi}} \exp\left(\hat{\delta}\gamma\right) \sum_{k=1}^{M} a_k \exp\left(b_k \hat{\beta}^2 q\right) E_{5,k}, \tag{72d}$$

$$E_{5,k} = \int_0^{q} x^{-3/2} \exp\left(-\frac{A_k^2}{2}x^{-1} - \frac{B_k^2}{2}x\right) dx. \tag{72e}$$

Using the substitution $u = x^{-1/2}$, E_3 can be rewritten as

$$\begin{aligned}E_3 &= 2\frac{\hat{\delta}}{\sqrt{2\pi}} \exp\left(\hat{\delta}\gamma\right) \int_0^{\frac{1}{\sqrt{q}}} \exp\left(-\frac{\hat{\delta}^2}{2}u^2 - \frac{\gamma^2}{2}u^{-2}\right) du \\ &= \frac{1}{2}\exp\left(\hat{\delta}\gamma\right)\left[\exp\left(\hat{\delta}\gamma\right)\operatorname{erf}(V_1) + \exp\left(-\hat{\delta}\gamma\right)\operatorname{erf}(V_2)\right. \\ &\quad \left. - \exp\left(\hat{\delta}\gamma\right) + \exp\left(-\hat{\delta}\gamma\right)\right] \\ &= \frac{1}{2}\left[1 + \operatorname{erf}(V_2)\right] - \frac{1}{2}\exp\left(2\hat{\delta}\gamma\right)\operatorname{erfc}(V_1).\end{aligned} \tag{73}$$

The second equality results from the formula [18]

$$\begin{aligned}&\int \exp\left(-a^2x^2 - b^2x^{-2}\right) dx \\ &= \frac{\sqrt{\pi}}{4a}\left[\exp(2ab)\operatorname{erf}\left(ax + bx^{-1}\right)\right. \\ &\quad \left. + \exp(-2ab)\operatorname{erf}\left(ax - bx^{-1}\right)\right] + c, \quad a \neq 0,\end{aligned}$$

where c is a constant. Similarly, $E_{4,k}$ and $E_{5,k}$ can be expressed as

$$\begin{aligned}E_{4,k} &= 2\int_0^{\frac{1}{\sqrt{q}}} \exp\left(-\frac{A_k^2}{2}u^2 - \frac{B_k^2}{2}u^{-2}\right) du \\ &= \frac{\sqrt{2\pi}}{2A_k}\left[\exp(A_k B_k)\operatorname{erf}(C_k) + \exp(-A_k B_k)\operatorname{erf}(D_k)\right. \\ &\quad \left. - \exp(A_k B_k) + \exp(-A_k B_k)\right] \\ &= \frac{\sqrt{2\pi}}{2A_k}\exp(-A_k B_k)\left[1 + \operatorname{erf}(D_k)\right] \\ &\quad - \frac{\sqrt{2\pi}}{2A_k}\exp(A_k B_k)\operatorname{erfc}(C_k),\end{aligned} \tag{74a}$$

$$\begin{aligned}E_{5,k} &= 2\int_{\frac{1}{\sqrt{q}}}^{+\infty} \exp\left(-\frac{A_k^2}{2}u^2 - \frac{B_k^2}{2}u^{-2}\right) du \\ &= \frac{\sqrt{2\pi}}{2A_k}\left[\exp(A_k B_k)\operatorname{erfc}(C_k)\right. \\ &\quad \left. + \exp(-A_k B_k)\operatorname{erfc}(D_k)\right],\end{aligned} \tag{74b}$$

respectively. Thus

$$-E_4 + E_5 = \frac{1}{2}\frac{\hat{\delta}}{\sqrt{2\pi}} \exp\left(\hat{\delta}\gamma\right) \sum_{k=1}^{M} a_k \exp\left(b_k \hat{\beta}^2 q\right)\left(E_{5,k} - E_{4,k}\right)$$

$$= \frac{1}{2}\hat{\delta}\exp\left(\hat{\delta}\gamma\right)\sum_{k=1}^{M}\frac{a_k}{A_k}\exp\left(q\hat{\beta}^2 b_k\right) \cdot \left[\exp\left(A_k B_k\right)\operatorname{erfc}\left(C_k\right) - \exp\left(-A_k B_k\right)\operatorname{erf}\left(D_k\right)\right]. \quad (75)$$

REFERENCES

[1] S. Chen and J. Zhao, "The requirements, challenges, and technologies for 5G of terrestrial mobile telecommunication," *IEEE Commun. Mag.*, vol. 52, no. 5, pp. 36–43, May 2014.

[2] X. Ge, H. Cheng, M. Guizani, and T. Han, "5G wireless backhaul networks: Challenges and research advances," *IEEE Netw.*, vol. 28, no. 6, pp. 6–11, Nov. 2014.

[3] C.-X. Wang *et al.*, "Cellular architecture and key technologies for 5G wireless communication networks," *IEEE Commun. Mag.*, vol. 52, no. 2, pp. 122–130, Feb. 2014.

[4] D. W. Matolak, "Probability density functions for SNIR in DS-CDMA," *IEEE Trans. Commun.*, vol. 57, no. 6, pp. 1628–1633, Jun. 2009.

[5] J. G. Andrews, R. K. Ganti, M. Haenggi, N. Jindal, and S. Weber, "A primer on spatial modeling and analysis in wireless networks," *IEEE Commun. Mag.*, vol. 48, no. 11, pp. 156–163, Nov. 2010.

[6] J. G. Andrews, F. Baccelli, and R. K. Ganti, "A tractable approach to coverage and rate in cellular networks," *IEEE Trans. Commun.*, vol. 59, no. 11, pp. 3122–3134, Nov. 2011.

[7] H.-S. Jo, Y. J. Sang, P. Xia, and J. G. Andrews, "Heterogeneous cellular networks with flexible cell association: A comprehensive downlink SINR analysis," *IEEE Trans. Wireless Commun.*, vol. 11, no. 10, pp. 3484–3495, Oct. 2012.

[8] S. Mukherjee, "Distribution of downlink SINR in heterogeneous cellular networks," *IEEE J. Sel. Areas Commun.*, vol. 30, no. 3, pp. 575–585, Apr. 2012.

[9] M. Di Renzo, A. Guidotti, and G. E. Corazza, "Average rate of downlink heterogeneous cellular networks over generalized fading channels: A stochastic geometry approach," *IEEE Trans. Commun.*, vol. 61, no. 7, pp. 3050–3071, Jul. 2013.

[10] H. S. Dhillon and J. G. Andrews, "Downlink rate distribution in heterogeneous cellular networks under generalized cell selection," *IEEE Wireless Commun. Lett.*, vol. 3, no. 1, pp. 42–45, Feb. 2014.

[11] 3GPP, "Evolved universal terrestrial radio access (EUTRA); further advancements for E-UTRA physical layer aspects," France, v9.0.0, TR 36.814, Mar. 2010.

[12] *IEEE* Standard for Air Interface for Broadband Wireless Access Systems, IEEE Standard 802.16, Aug. 2012.

[13] H. Tabassum, Z. Dawy, M.-S. Alouini, and F. Yilmaz, "A generic interference model for uplink OFDMA networks with fractional frequency reuse," *IEEE Trans. Veh. Technol.*, vol. 63, no. 3, pp. 1491–1497, Mar. 2014.

[14] M. Ahmadi, M. Ni, and J. Pan, "A geometrical probability-based approach towards the analysis of uplink inter-cell interference," in *Proc. IEEE GLOBECOM*, Dec. 2013, pp. 4952–4957.

[15] Y. Zhuang, Y. Luo, L. Cai, and J. Pan, "A geometric probability model for capacity analysis and interference estimation in wireless mobile cellular systems," in *Proc. IEEE GLOBECOM*, Dec. 2011, pp. 1–6.

[16] K. A. Hamdi, "On the statistics of signal-to-interference plus noise ratio in wireless communications," *IEEE Trans. Commun.*, vol. 57, no. 11, pp. 3199–3204, Nov. 2009.

[17] N. Mehta, J. Wu, A. Molisch, and J. Zhang, "Approximating a sum of random variables with a lognormal," *IEEE Trans. Wireless Commun.*, vol. 6, no. 7, pp. 2690–2699, Jul. 2007.

[18] M. Abramowitz and I. A. Stegun, *Handbook of Mathematical Functions With Formulas, Graphs, and Mathematical Tables*, 9th ed. New York, NY, USA: Dover, 1972.

[19] L. F. Fenton, "The sum of log-normal probability distributions in scatter transmission systems," *IRE Trans. Commun. Syst.*, vol. 8, no. 1, pp. 57–67, Mar. 1960.

[20] S. C. Schwartz and Y.-S. Yeh, "On the distribution function and moments of power sums with log-normal components," *Bell Syst. Tech. J.*, vol. 61, no. 7, pp. 1441–1462, Sep. 1982.

[21] N. C. Beaulieu and Q. Xie, "An optimal lognormal approximation to lognormal sum distributions," *IEEE Trans. Veh. Technol.*, vol. 53, no. 2, pp. 479–489, Mar. 2004.

[22] H. Nie and S. Chen, "Lognormal sum approximation with type IV Pearson distribution," *IEEE Commun. Lett.*, vol. 11, no. 10, pp. 790–792, Oct. 2007.

[23] M. D. Renzo, F. Graziosi, and F. Santucci, "Further results on the approximation of log-normal power sum via Pearson type IV distribution: A general formula for log-moments computation," *IEEE Trans. Commun.*, vol. 57, no. 4, pp. 893–898, Apr. 2009.

[24] Q. Zhang and S. Song, "A systematic procedure for accurately approximating lognormal-sum distributions," *IEEE Trans. Veh. Technol.*, vol. 57, no. 1, pp. 663–666, Jan. 2008.

[25] M. D. Renzo and F. Graziosi, "Approximating the linear combination of log-normal RVs via pearson type IV distribution for UWB performance analysis," *IEEE Trans. Commun.*, vol. 57, no. 2, pp. 388–403, Feb. 2009.

[26] K. W. Sung, H. Haas, and S. McLaughlin, "A semianalytical PDF of downlink SINR for femtocell networks," *EURASIP J. Wireless Commun. Netw.*, vol. 2010, no. 5, pp. 1–9, Jan. 2010.

[27] M. Renzo, F. Graziosi, and F. Santucci, "A comprehensive framework for performance analysis of cooperative multi-hop wireless systems over log-normal fading channels," *IEEE Trans. Commun.*, vol. 58, no. 2, pp. 531–544, Feb. 2010.

[28] C. Lam and T. Le-Ngoc, "Log-shifted Gamma approximation to log-normal sum distributions," *IEEE Trans. Veh. Technol.*, vol. 56, no. 4, pp. 2121–2129, Jul. 2007.

[29] L. Zhao and J. Ding, "Least squares approximations to lognormal sum distributions," *IEEE Trans. Veh. Technol.*, vol. 56, no. 2, pp. 991–997, Mar. 2007.

[30] A. Eriksson, E. Ghysels, and F. Wang, "The normal inverse Gaussian distribution and the pricing of derivatives," *J. Deriv.*, vol. 16, no. 3, pp. 23–37, Jan. 2009.

[31] A. Hyvärinen, J. Karhunen, and E. Oja, *Independent Component Analysis*. Hoboken, NJ, USA: Wiley, 2004.

[32] 3GPP, "Universal mobile telecommunications system (UMTS); spacial channel model for multiple input multiple output (MIMO) simulations," France, v9.0.0, TR 125 996, Jan. 2010.

[33] G. T. F. de Abreu, "Jensen-Cotes upper and lower bounds on the Gaussian Q-function and related functions," *IEEE Trans. Commun.*, vol. 57, no. 11, pp. 3328–3338, Nov. 2009.

[34] A. Eriksson, E. Ghysels, and L. Forsberg, *Approximating the Probability Distribution of Functions of Random Variables: A New Approach*. Montréal, Quéc, Canada: Cirano, 2004.

[35] C. Charlier, *Über die darstellung willkürlicher funktionen*. Stockholm and Uppsala, Sweden: Almqvist & Wilksells Boktryckeri AB, 1905.

[36] F. Edgeworth, "On the representation of statistical frequency by a series," *J. Roy. Stat. Soc.*, vol. 70, no. 1, pp. 102–106, Mar. 1907.

[37] O. E. Barndorff-Nielsen, "Processes of normal inverse Gaussian type," *Finance Stochastics*, vol. 2, no. 1, pp. 41–68, Nov. 1997.

[38] O. Olabiyi and A. Annamalai, "New exponential-type approximations for the erfc (.) and erfc^p (.) functions with applications," in *Proc. IEEE Int. Wireless Commun. Mobile Comput. Conf. (IWCMC)*, Aug. 2012, pp. 1221–1226.

[39] D. N. Gujarati, *Basic Econometrics*, 4th ed. New York, NY, USA: McGraw-Hill, 2003.

[40] A. A. Abu-Dayya and N. C. Beaulieu, "Outage probabilities in the presence of correlated lognormal interferers," *IEEE Trans. Veh. Technol.*, vol. 43, no. 1, pp. 164–173, Feb. 1994.

[41] T. M. Cover and J. A. Thomas, *Elements of Information Theory*. Hoboken, NJ, USA: Wiley, 1991.

[42] S. Fan, "A new extracting formula and a new distinguishing means on the one variable cubic equation," *Nat. Sci. J. Hainan Teach. Coll.*, vol. 2, no. 2, pp. 91–98, Dec. 1989.

Xiaojun Yan received the B.Eng. degree in communications engineering from the Wuhan University of Technology, Wuhan, China, in 2011. He is currently pursuing the Ph.D. degree in communications and information systems at the Shanghai Institute of Microsystem and Information Technology (SIMIT), Chinese Academy of Sciences (CAS), Shanghai, China. His research interests include the statistical analysis and modeling of wireless networks.

Jing Xu received the M.S. degree in electronic engineering from Jilin University, Chang Chun, China, and the Ph.D. degree in radio engineering from Southeast University, Nanjing, China, in 2001 and 2005, respectively. He is a Professor with Shanghai Institute of Microsystem and Information Technology (SIMIT), Chinese Academy of Sciences (CAS), Shanghai, China, and obtained the Shanghai Young Rising Star (2010). His research interests include intercell interference mitigation, interference modeling, co-operative communications, and software-defined wireless networks.

Yuanping Zhu received the B.Eng. degree in electronic information science and technology from the Wuhan University, Wuhan, China, and the Ph.D. degree in communications and information systems from the Shanghai Institute of Microsystem and Information Technology (SIMIT), Chinese Academy of Sciences (CAS), Shanghai, China, in 2008 and 2013, respectively. She is currently an Assistant Professor with the SIMIT, CAS. Her research interests include wireless resource allocation and statistical modeling for wireless networks.

Jiang Wang received the B.S. and M.S. degrees from the University of Electronic Science and Technology of China, Chengdu, China, and the Ph.D. degree from Southeast University, Nanjing, China, in 1998, 2001, and 2006, respectively. He joined the 4G Department, Shanghai Institute of Microsystem and Information Technology, in June 2006, as a Research Assistant and has been an Associate Professor from January 2010. As a Project Manager/Subtopic Manager responsible for the Key National project, the Basic Research project of Shanghai, and the collaboration project of WiCO, he has authored or coauthored over 10 technical papers published in journals and conferences, and over 15 pending patents, including 12 PCT patents. His research interests include single frequency networking for future wireless communication systems, radio resource management, cross-layer optimization, B4G/5G architecture design, and standardization.

Yang Yang (SM'10) received the B.Eng. and M.Eng. degrees in radio engineering from Southeast University, Nanjing, China, and the Ph.D. degree in information engineering from the Chinese University of Hong Kong, Hong Kong, in 1996, 1999, and 2002, respectively. He is currently a Professor with the School of Information Science and Technology, ShanghaiTech University, Shanghai, China, and the Director of Shanghai Research Center for Wireless Communications (WiCO), Shanghai, China. Prior to that, he has served as a Professor with Shanghai Institute of Microsystem and Information Technology (SIMIT), Chinese Academy of Sciences, Shanghai, China, a Senior Lecturer with the Department of Electronic and Electrical Engineering, University College London (UCL), London, U.K., a Lecturer with the Department of Electronic and Computer Engineering, Brunel University, Uxbridge, U.K., and an Assistant Professor with the Department of Information Engineering, Chinese University of Hong Kong, Hong Kong. His research interests include wireless ad hoc and sensor networks, wireless mesh networks, next generation mobile cellular systems, intelligent transport systems, and wireless testbed development and practical experiments. He has coedited a book, *Heterogeneous Cellular Networks* (Cambridge University Press, 2013) and coauthored more than 100 technical papers. He has served on the organization teams of about 50 international conferences including as a Co-Chair of Ad-hoc and Sensor Networking Symposium at the IEEE ICC 15, and Communication and Information System Security Symposium at the IEEE GLOBECOM'15.

Cheng-Xiang Wang (S'01–M'05–SM'08) received the B.Sc. and M.Eng. degrees in communication and information systems from Shandong University, Jinan, China, and the Ph.D. degree in wireless communications from Aalborg University, Aalborg, Denmark, in 1997, 2000, and 2004, respectively. He has been with Heriot-Watt University, Edinburgh, U.K., since 2005, and was promoted to a Professor of wireless communications in 2011. He was a Research Fellow with the University of Agder, Grimstad, Norway, from 2001 to 2005, a Visiting Researcher at Siemens AG-Mobile Phones, Munich, Germany, in 2004, and a Research Assistant with Technical University of Hamburg-Harburg, Hamburg, Germany, from 2000 to 2001. His research interests include wireless channel modelling and 5G wireless communication networks. He has edited one book and published over 230 papers in refereed journals and conference proceedings. He served or is currently serving as an Editor for nine international journals, including the IEEE TRANSACTIONS ON VEHICULAR TECHNOLOGY (since 2011), the IEEE TRANSACTIONS ON COMMUNICATIONS (since 2015), and the IEEE TRANSACTIONS ON WIRELESS COMMUNICATIONS (2007–2009). He was the leading Guest Editor for the IEEE JOURNAL ON SELECTED AREAS IN COMMUNICATIONS (special issue on Vehicular Communications and Networks). He served or is serving as a TPC member, the TPC Chair, and the General Chair for over 80 international conferences. He is a Fellow of the IET, a Fellow of the HEA, and a member of EPSRC Peer Review College. He was the recipient of best paper awards from the IEEE GLOBECOM 2010, the IEEE ICCT 2011, the ITST 2012, the IEEE VTC 2013-Spring, and the IWCMC 2015.